

THE LOCAL SUPERCLUSTER

R. BRENT TULLY

Institute for Astronomy, University of Hawaii

Received 1981 August 21; accepted 1981 December 3

ABSTRACT

An attempt is made to illustrate the three-dimensional distribution of nearby galaxies. There is an evident overdensity of galaxies in the north galactic hemisphere that has been called the Local Supercluster. It is argued that this system comprises two distinct components: a disk component with 60% of the luminous galaxies, and a halo component with 40% of the luminous galaxies. With regard to the halo component, (i) almost all luminous galaxies are associated with only a small number of clouds, (ii) as a consequence, most of the volume off the disk of the Local Supercluster is empty, (iii) the clouds in the halo are sufficiently separated from the disk so that the two-component distinction seems warranted, and (iv) at least the more prominent clouds in the halo seem to be prolate structures with their long axes directed toward the Virgo Cluster. This elongated structure may be attributed to tidal effects that were important at the epoch of the formation of the halo clouds. A tentative limit for the date of that epoch is $z \lesssim 8$.

With regard to the disk component, (i) the ratio of the longest to the shortest axis is 6 to 1 (practically independent of velocity effects), and (ii) the absolute rms dimension of the short axis is $\pm 1.1 h^{-1} \text{ Mpc}$ ($h = H_0/100 \text{ km s}^{-1} \text{ Mpc}^{-1}$). For the disk component to be so thin either (i) we are viewing the disk at the moment of collapse, (ii) there is a great deal of unseen matter in the disk, or (iii) random motions normal to the disk are less than 100 km s^{-1} . If velocities normal to the plane of the Local Supercluster are very low, the implication would be that the disk was formed through dissipative processes.

The thinness of the disk of the supercluster, the extreme segregation of galaxies into a small fraction of the volume available, and the low local random motions are all evidence which weigh against gravitational clustering models in which galaxies formed before superclusters and in favor of the viewpoint that galaxies fragmented out of larger scale structure.

Subject headings: cosmology — galaxies: clusters of

I. A HISTORICAL PERSPECTIVE AND NEW DATA

It is well known that there is a marked excess of relatively nearby galaxies in the vicinity of the north galactic pole. De Vaucouleurs (1953, 1956) coined the terminology Local Supercluster to describe this structure which extends over 90° or more and which contains within it concentrations such as the Virgo Cluster and several tens of small groups. From the earliest papers on this subject by de Vaucouleurs to his most recent (de Vaucouleurs 1975*b, c, d*, 1976*a*) the point has been made that the distribution of galaxies in the Local Supercluster is quite flattened. In the two Reference Catalogues (de Vaucouleurs and de Vaucouleurs 1964; de Vaucouleurs, de Vaucouleurs, and Corwin 1976), supergalactic coordinates (SGL, SGB) are defined in terms of this apparent plane.

However, although these ideas have been around for some time, the properties of the Local Supercluster have remained poorly understood. For example, Bahcall and Joss (1976) have argued that, granted the Virgo Cluster

exists and granted there exists structure at lower density contrast on scales of 5° or less, the apparent flattened distribution of galaxies on the plane of the sky could be the illusory consequence of a chance projected alignment of the Virgo Cluster and a small number of secondary clusters or groups.

This particular controversy will surely dissolve with the much improved statistics provided by recent redshift surveys and with the close scrutiny provided by information about the distribution of galaxies in the third dimension. The two most important redshift surveys for the present discussion are those of Sandage (1978), which ensures completion to the specific magnitude limit of the Shapley-Ames (1932) catalog, and Fisher and Tully (1981), which provides flesh to earlier skeletal views by providing information on the many minor systems that swarm about the few luminous giants. In all, some 2200 galaxies now have measured systemic velocities of less than 3000 km s^{-1} (adjusted for solar motion of 300 km s^{-1} toward $l = 90^\circ$, $b = 0^\circ$), a velocity corresponding to roughly three times the distance to the

Virgo Cluster and twice the distance to my putative edge to the Local Supercluster. A compendium of the optical and H I properties of this sample and maps illustrating the distribution of these objects on the sky will be published as the *Atlas and Catalog of Nearby Galaxies* (Tully and Fisher 1982; hereafter NBG).

The present discussion is preliminary because, throughout, the assumption will be made that there are no departures from a uniform Hubble expansion. It is almost certain that this viewpoint is naive; that, at the least, we have a peculiar motion toward the Virgo Cluster of several hundred kilometers per second (de Vaucouleurs 1976*b*; Aaronson *et al.* 1980, 1982; Schechter 1980; Tonry 1980). However, it will be shown that there are a number of very basic properties of the distribution of nearby galaxies that can be deduced independent of accurate line-of-sight distances.

II. THE SUPERCLUSTER IN THREE DIMENSIONS

All galaxies in the nearby galaxies sample (NBG) can be mapped in three dimensions with the assumption of a strictly linear relationship between redshifts and distances ($H_0 = 100 h \text{ km s}^{-1} \text{ Mpc}^{-1}$). A useful coordinate system will be Cartesian supergalactic coordinates, (SGX, SGY, SGZ), derivative of the polar coordinates (SGL, SGB, distance). The SGZ axis is defined to point in the direction $\text{SGB} = +90^\circ$; the SGX axis is aligned toward $\text{SGL} = 0^\circ$, $\text{SGB} = 0^\circ$; and the SGY axis is aligned toward $\text{SGL} = 90^\circ$, $\text{SGB} = 0^\circ$. The positive SGY axis is only 6° removed from the north galactic pole, and the SGX-SGZ plane is almost coincident with the plane of the Galaxy. The Virgo Cluster is 13° from the SGY axis. It is very convenient that our Galaxy is almost face-on to viewers who live near the center of the Local Supercluster.

All galaxies in NBG are plotted in Figures 1–3, three orthogonal projections of a spherical volume of radius $30 h^{-1} \text{ Mpc}$.¹ The overdensity of nearby galaxies in the north galactic hemisphere and their flattened distribution are readily apparent. In Figure 1 there is a suggestion of a secondary stratum parallel to the principal plane at $\text{SGZ} \approx -2.5 h^{-1} \text{ Mpc}$. Two points must be emphasized: (i) there is seldom a significant velocity component in SGZ when SGZ is small, and (ii) a scale length of roughly a megaparsec for the dropoff in the number density of galaxies normal to the apparent plane is an order of magnitude smaller than could be anticipated if the cause were galactic absorption. The flattened distribution is *not* an artifact of velocity effects, incompleteness, or obscuration.

¹Galaxies superposed upon a 6° radius Virgo Cluster and a 3° radius Fornax Cluster are assigned common distances ($10.7 h^{-1} \text{ Mpc}$ and $13.4 h^{-1} \text{ Mpc}$, respectively), with sufficient dispersion that the clusters have similar dimensions in the line of sight and on the plane of the sky.

Axial symmetry with respect to the Virgo Cluster might have been anticipated, but there is little suggestion in the polar view (Fig. 2) that such a distribution is the case. We need to be careful now because velocity streaming and incompleteness with increasing distance must distort our view. However, the more detailed inspection which follows will sustain this initial impression that the Local Supercluster viewed face-on would appear very asymmetric.

Whatever the effects of non-Hubble motions, there is an unavoidable bias in Figures 1–3 as a consequence of incompleteness as a function of distance. A more accurate picture emerges if a sample is defined in terms of a cutoff in intrinsic luminosity, chosen so that the sample will be *complete* within a specified volume. With the Sandage (1978) data included, there is redshift information for essentially the entire Shapley-Ames sample of galaxies. This magnitude-limited sample is complete for galaxies brighter than $\sim 12.7 \text{ mag}$ on the Harvard scale (Sandage and Tammann 1981). Upon correcting for inclination and galactic absorption effects, the completeness limit becomes $B_T^{b,i} \approx 12.0 \text{ mag}$.²

The region of enhanced density in the northern galactic hemisphere that is evident in Figures 1–3 and in the stereoscopic projections published by Yahil, Sandage, and Tammann (1980) is roughly enclosed by the limits:

$$\begin{aligned} -10 h^{-1} < \text{SGX} < +10 h^{-1} \text{ Mpc} \\ 0 < \text{SGY} < +15 h^{-1} \text{ Mpc} \\ -10 h^{-1} < \text{SGZ} < +10 h^{-1} \text{ Mpc.} \end{aligned}$$

All unobscured galaxies in this volume brighter than $M_B^{b,i} = -19 + 5 \log h$ should be known, except in the corners (galaxies with $B_T^{b,i} = 12.0$ and $M_B^{b,i} = -19 + 5 \log h$ will be situated at $\mu_0 = 31.0 + 5 \log h$, or $D = 15.9 h^{-1} \text{ Mpc}$. The extreme corners of the volume are at $\mu_0 = 31.6 + 5 \log h$, or $D = 20.6 h^{-1} \text{ Mpc}$). In the following discussion this “complete” sample will be supplemented by one extending a magnitude fainter. The “extended” sample will provide better statistics and is largely complete over most of the volume.

With distances determined from redshifts, there are 125 galaxies brighter than $-19 + 5 \log h$, and 334 galaxies brighter than $-18 + 5 \log h$ in the volume that has been defined. Of these, 25 and 62, respectively, are in the 6° radius core of the Virgo Cluster. Only 20% of the

²The adjustment from Harvard to total blue magnitudes depends in a complicated way on major and minor dimensions and morphological type, but there is no significant zeroth-order scale correction. An essentially complete sample is available to $B_T^{b,i} \approx 12.0 \text{ mag}$ for those galaxies with inclination corrections, A_i , plus galactic absorption corrections, A_b , less than $\sim 0.7 \text{ mag}$. With the corrections proposed by Fisher and Tully (1981), the maximum tilt correction is $A_i = 1.08 \text{ mag}$ and, as long as $|b| > 30^\circ$, then $A_b < 0.3 \text{ mag}$, so incompleteness among galaxies brighter than $B_T^{b,i} = 12.0 \text{ mag}$ will be very slight.

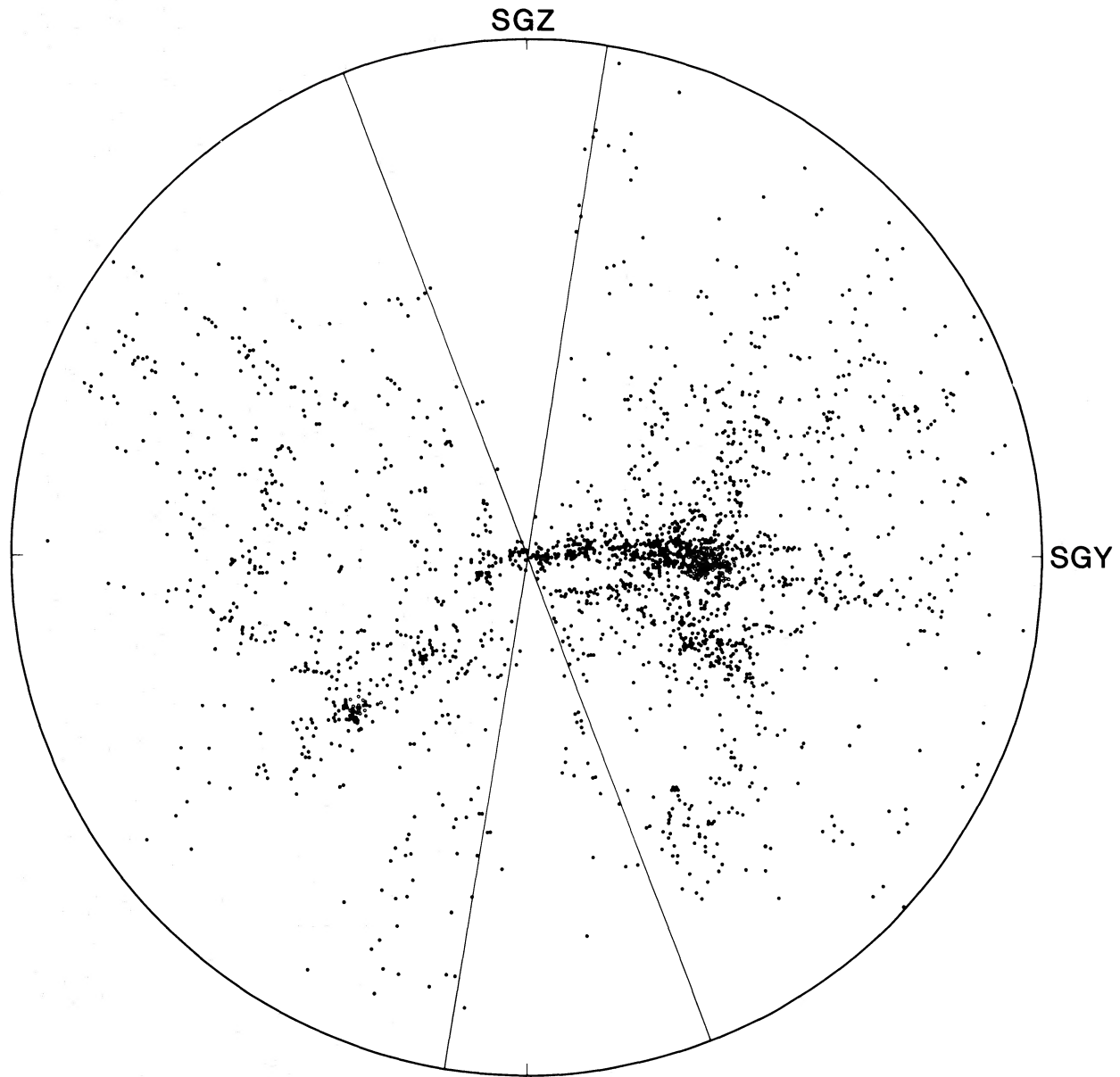


FIG. 1.—All 2175 galaxies in the NBG catalog projected onto the SGY-SGZ plane. Three-dimensional positions have been computed assuming a uniformly expanding universe and $H_0 = 100 h \text{ km s}^{-1} \text{ Mpc}^{-1}$. Galaxies associated with a 6° Virgo Cluster and a 3° Fornax Cluster (*open circles*) are located at common distances, plus or minus sufficient dispersion to give the clusters a spherical appearance. The radius of the outer boundary is $30 h^{-1} \text{ Mpc}$. The galactic zone of avoidance ($|b| < 15^\circ$) is contained within the opposed wedges tilted by 6° with respect to the SGZ axis. There is a zone of incompleteness ($\delta < -45^\circ$) which is projected across most of the southern supergalactic hemisphere.

most luminous galaxies associated with the Local Supercluster are in the Virgo Cluster.

As de Vaucouleurs has noted and as was evident in Figure 1, nearby galaxies in the northern galactic hemisphere tend to lie in a plane normal to the SGZ axis. This property is illustrated in a striking manner in Figure 4, which shows the SGZ distribution of all galaxies more luminous than $-18 + 5 \log h$ in the region

of the Local Supercluster ($0 < \text{SGY} < 15 h^{-1} \text{ Mpc}$; $|\text{SGX}| < 10 h^{-1} \text{ Mpc}$), *excluding* members of the Virgo Cluster. Note that the decrease in the number density of galaxies with distance from the $\text{SGZ} = 0$ plane is on a scale an order of magnitude smaller than would be expected if galactic obscuration were the cause.

The provocative question evoked by Figure 4 is whether it would be justifiable to represent the distribu-

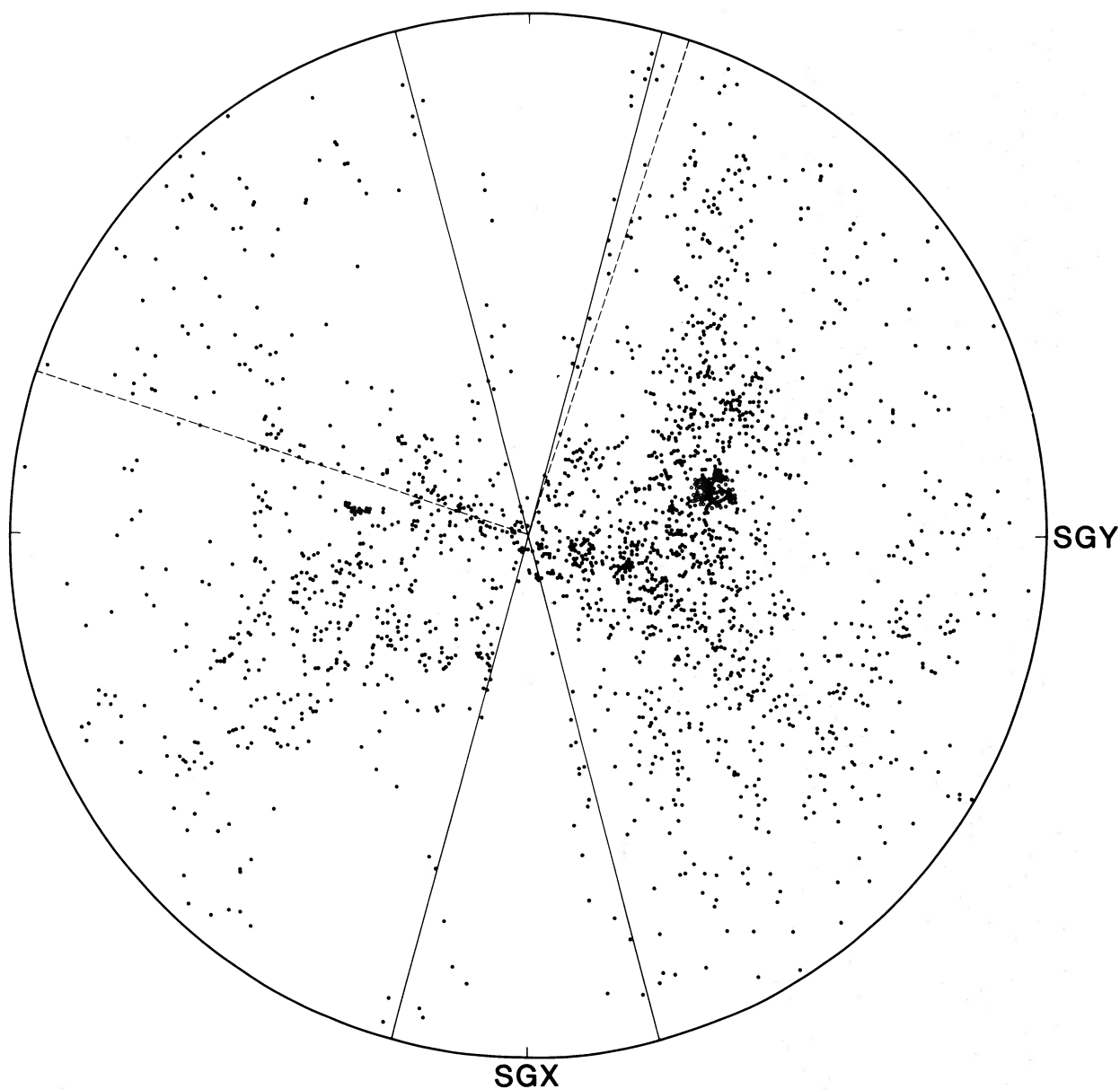


FIG. 2.—All galaxies in the NBG catalog projected onto the SGX–SGY plane. The galactic zone of avoidance is symmetric about the SGX axis. The large wedge occupying the upper left quadrant locates the zone of incompleteness.

tion normal to the apparent plane in terms of two components: one component with a scale height of roughly $1 h^{-1}$ Mpc, and the other component extending over a scale height comparable with the orthogonal dimensions of the supercluster. If galaxies associated with the 6° radius Virgo Cluster are excluded from consideration, the two components would contain roughly equal fractions of the luminous galaxies in the supercluster. Further on, it will be argued that the two component description has some physical sense.

In order to illustrate the distribution of nearby galaxies in greater detail, the three-dimensional volume defined above and encompassing the Local Supercluster is shown via a series of slices in Figures 5 and 6. These slices are taken in planes normal to the SGZ axis, i.e., parallel to the plane of the Local Supercluster. In Figure 5, the slices are $2 h^{-1}$ Mpc thick. The projected location of galaxies residing within each slice are mapped, using symbols coded by intrinsic luminosity. The same volume is dissected in Figure 6, but now the slices are $1 h^{-1}$

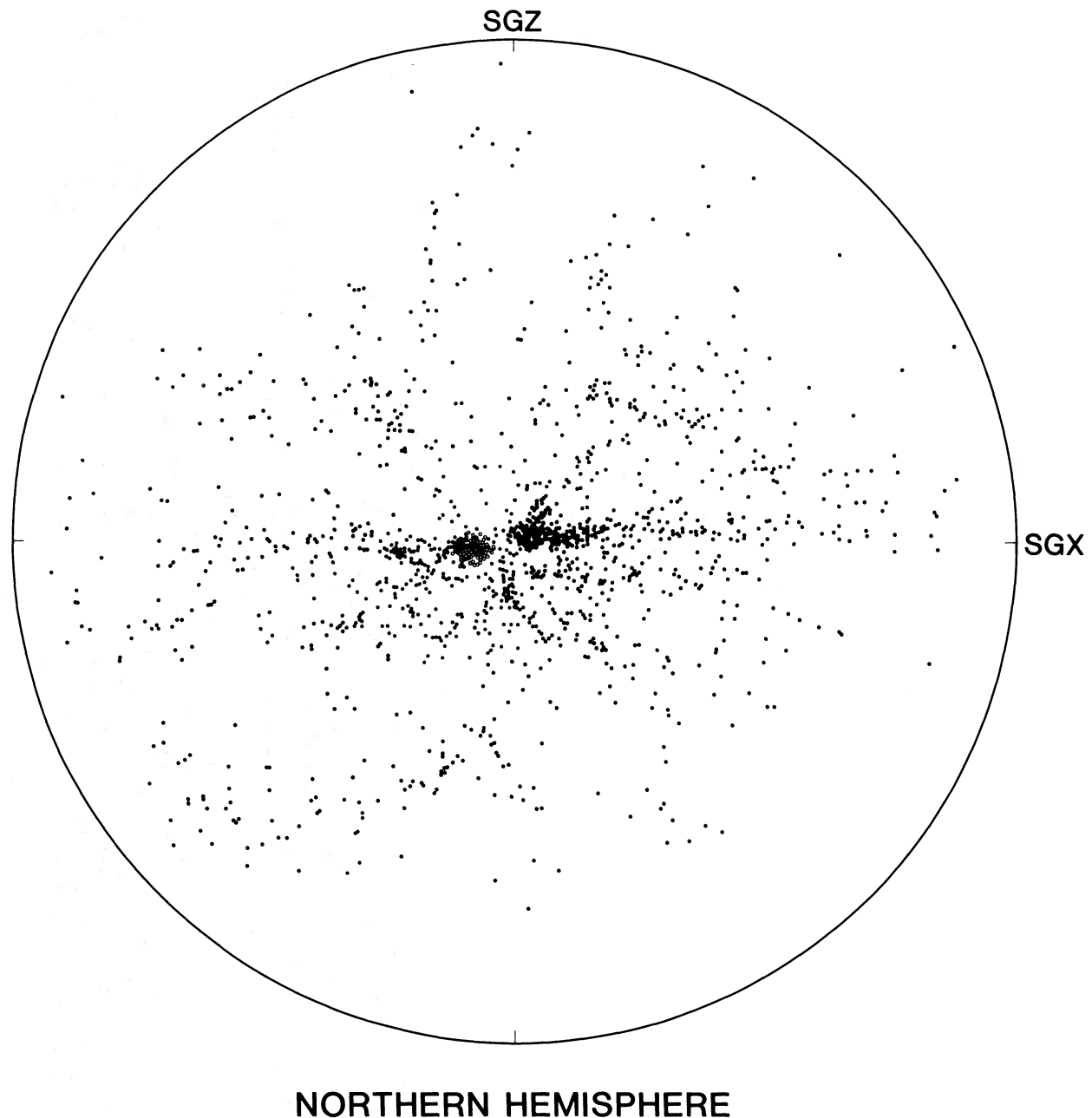


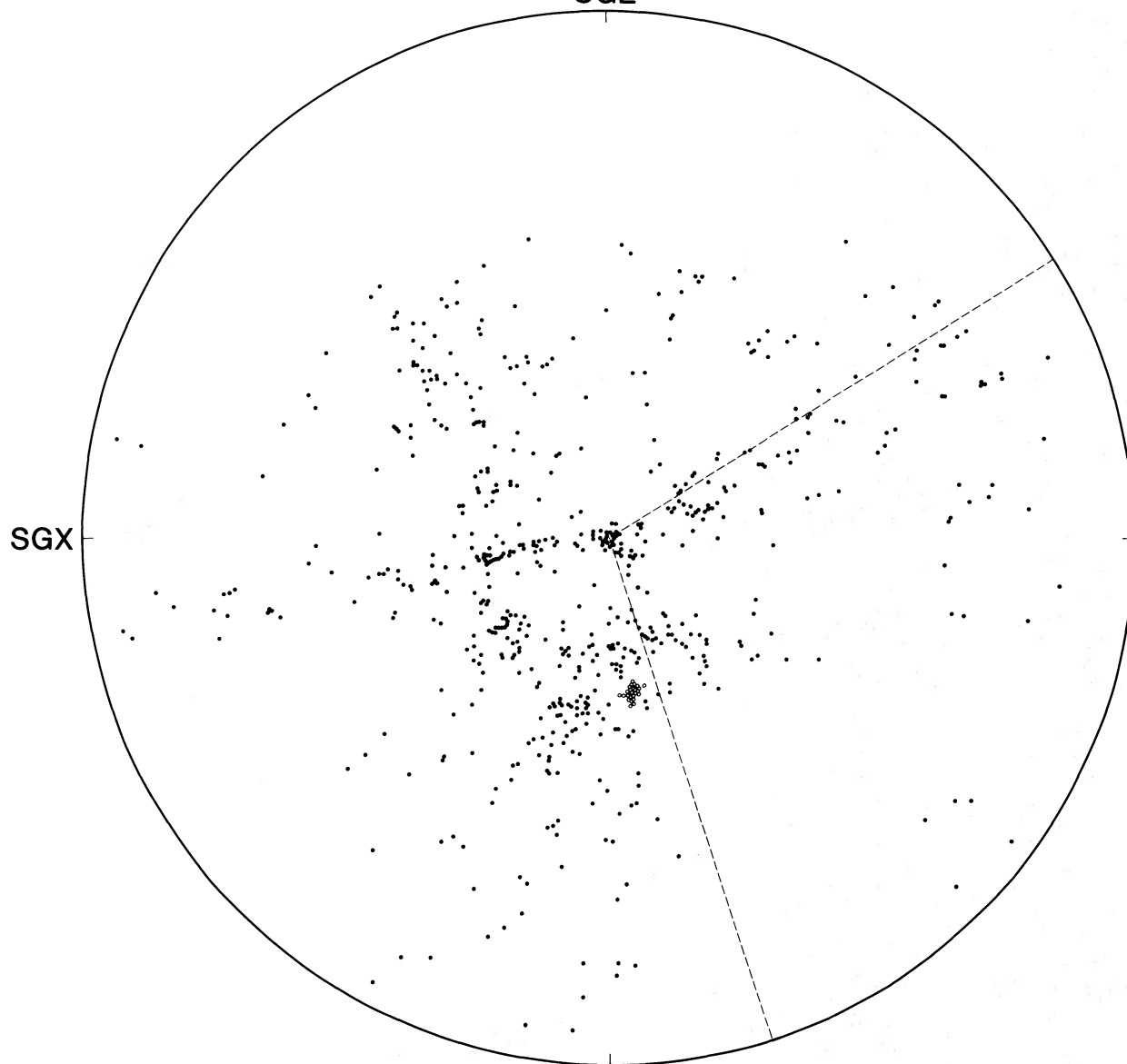
FIG. 3a

FIG. 3.—(a) All 1529 galaxies in the NBG catalog in the *north* galactic hemisphere ($SGY > 0$) projected onto the SGX–SGZ plane. The effect of obscuration increases with radius ρ , according to the relationship $\rho/[1-\rho^2]^{1/2}$, where ρ is in units of the maximum radius: $0 \leq \rho \leq 1$. (b) All 646 galaxies in the NBG catalog in the *south* galactic hemisphere ($SGY < 0$) projected onto the SGX–SGZ plane. The effect of obscuration is the same as in Fig. 3a. The zone of incompleteness is indicated.

Mpc thick and different symbols are used to suggest associations with distinct structures.

The remarkable fact is that most of the luminous galaxies in the Local Supercluster do lie within only a small number of discrete structures and, consequently, most of the volume in this relatively crowded region is

quite empty. Aside from the moderately rich and compact Virgo Cluster, the discrete structures are sufficiently extended and random motions are sufficiently modest (see § Vb) that crossing times today are generally substantially longer than the age of the universe. Such entities will be called clouds, in the spirit of



SOUTHERN HEMISPHERE

FIG. 3b

de Vaucouleurs (1975*a*) nomenclature (and consistent with that nomenclature whenever possible). Within clouds, as substructure, is a multitude of small groups which are characterized by crossing times less than or comparable to a Hubble time. The properties of this small scale structure are not of concern for the present discussion. The principal clouds that collectively constitute the Local Supercluster are identified in Table 1.

A point that deserves emphasis at this juncture is that most of the entities that have been identified in Table 1

are clearly separated in projection on the sky and, consequently, there need be little concern that we are being misled by kinematic effects that might enter the line-of-sight component to positions. The *plane-of-sky* distribution of the "complete" and "extended" samples of galaxies is shown in Figure 7. The distribution is shown without editorial comment in Figure 7*a*, while symbols indicate cloud assignments in Figure 7*b*. It can be seen that with no more distance information than that necessary to discriminate against background ob-

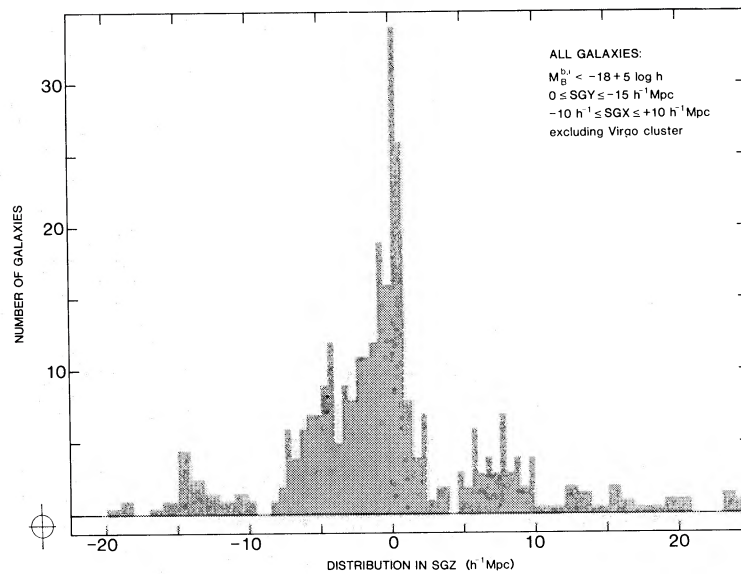


FIG. 4.—The distribution of galaxies normal to the plane of the Local Supercluster. The histogram illustrates the SGZ distribution of all galaxies with $-10 < SGX < +10 h^{-1} \text{ Mpc}$, $0 < SGY < +15 h^{-1} \text{ Mpc}$, and $M_B^{b,i} < -18 + 5 \log h$, excluding galaxies associated with the 6° Virgo Cluster.

jects ($V_0 > 1500 \text{ km s}^{-1}$) or low luminosity foreground objects ($M_B^{b,i} > -18 + 5 \log h$) there is already a clean separation between the clouds associated with the plane of the supercluster and those that are not. Virgo III, Crater, Antlia, and Draco are all seen as distinct entities. Leo I, Leo II, and Leo Minor are separated from all other structure, but the three cannot be decoupled from each other without velocity information.

The three most substantial of the clouds in Table 1 (plus the rather insignificant NGC 5643 Group) lie in a common plane: de Vaucouleurs' supergalactic plane. It is not of great consequence to the thesis of this paper if the two extended clouds Virgo II and Canes Venatici (CVn) are not, in fact, distinct entities. In defense of my description, the apparent void between these two clouds is distinguished on the plane of the sky (see Fig. 7) and, consequently, is insensitive to distance assignments. The Virgo Cluster (de Vaucouleurs' Virgo I) is likewise sufficiently separated on the plane of the sky from the CVn Cloud. The separation between the Virgo Cluster and the Virgo II Cloud is much less clear-cut. It was argued by Tully and Fisher (1977; see also de Vaucouleurs and de Vaucouleurs 1973) that these entities are distinct. Their argument can be summarized as follows. Within the 6° radius core of the Virgo Cluster, velocity dispersions are high ($\sigma \sim 700 \text{ km s}^{-1}$) and well mixed in the sense that there is no significant segregation of galaxies on the plane of the sky in any particular velocity interval. By contrast, quite abruptly beyond 6° radius, there is a marked segregation of galaxies in specific velocity intervals as if there were three or four groups, each with low internal dispersion ($\sigma \sim 100 \text{ km s}^{-1}$), seen in projec-

tion just off the edge of the Virgo Cluster. Each of these groups would be, in fact, subcomponents of the Virgo II Cloud. While I think these arguments are persuasive, it is not really important for the present discussion whether the Virgo Cluster and the clouds that define the plane of the Local Supercluster are actually clearly separated.

So, some 60% of the luminous galaxies in the volume enclosing the Local Supercluster are accounted for within the structure that defines the plane of the supercluster: 20% are in the Virgo Cluster itself and 40% lie within the two flattened clouds Virgo II and CVn. Most of the remaining 40% lie within only five clouds off the plane of the supercluster. *Most of the volume off the supergalactic plane is a great void.*

Consider first the north supergalactic pole. The only entities identified in this volume are the Virgo III Cloud and the almost inconsequential Draco Cloud. In the interval $3 h^{-1} \text{ Mpc} < SGZ < 10 h^{-1} \text{ Mpc}$, a volume³ of $2100 h^{-3} \text{ Mpc}^3$, there are only four luminous galaxies that do *not* lie in either of these two clouds.

Each cloud can be ascribed a volume defined by the shell of a triaxial spheroid with axes related to the rms separation of galaxies from the cloud center along three orthogonal axes. The 2σ dimensions of clouds in the supercluster are quoted in Table 1. If the radial distribution of galaxies can be assumed to be Gaussian (not a bad approximation), then 95% of galaxies associated with a cloud will be within the 2σ shell. Even with this rather generous definition, the two clouds, Virgo III and Draco, occupy only 250 Mpc^3 , or $\sim 16\%$ of the absorp-

³Galactic obscuration affects our view of $\sim 30\%$ of this volume.

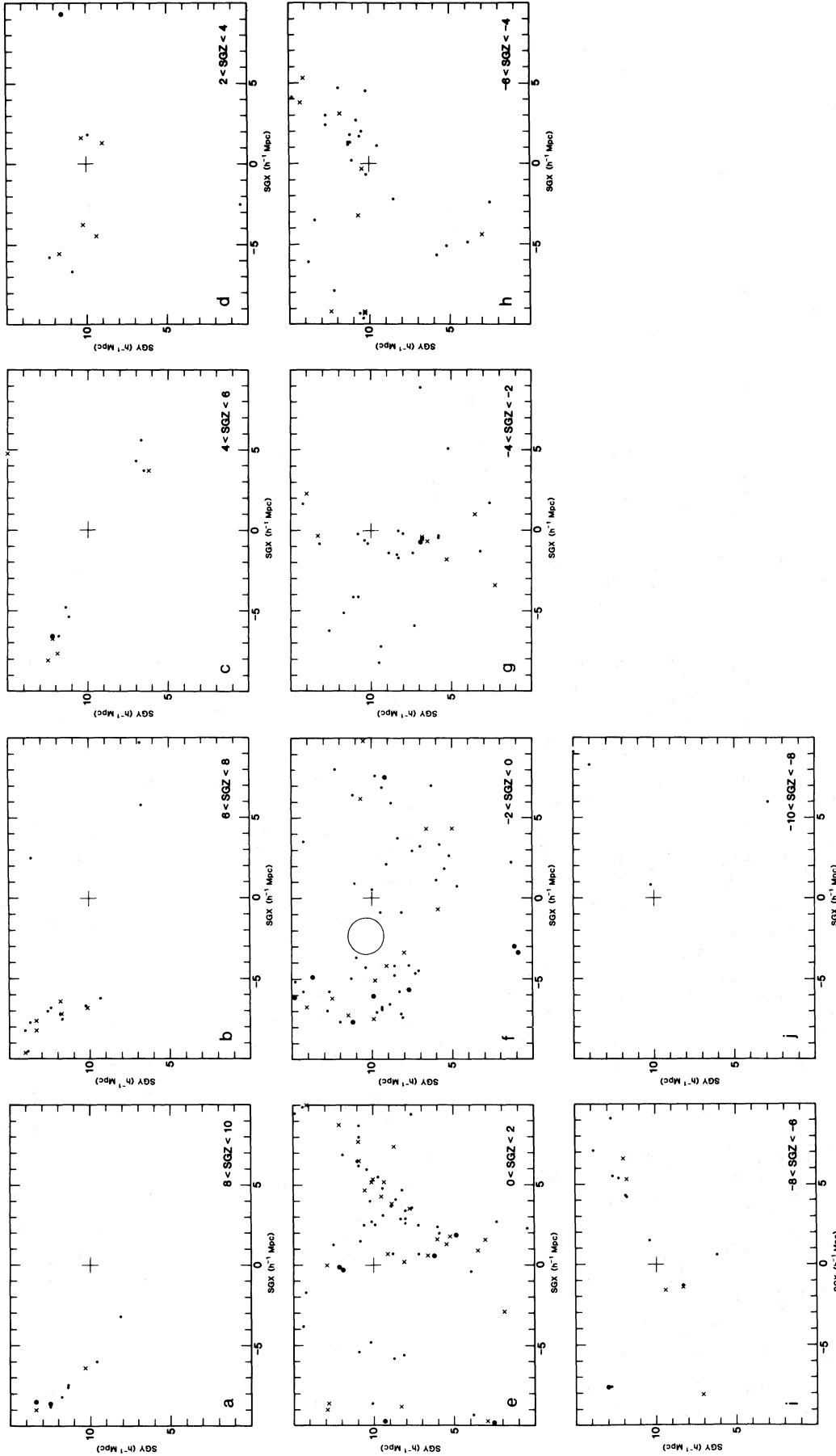


FIG. 5.—The Local Supercluster viewed by sections. Symbols indicate the projected locations of galaxies within individual $2 h^{-1} \text{ Mpc}$ thick slabs oriented parallel to the plane. Galaxies drawn from the “complete” sample are represented by large filled circles (if brighter than $-20 + 5 \log h$) or crosses, while galaxies associated with the “extended” sample are represented by small dots. The 62 galaxies associated with the 6° Virgo Cluster are not plotted individually, but would all lie within the ring of radius $1.1 h^{-1} \text{ Mpc}$ centered at $\text{SGX} = -2.4$, $\text{SGY} = 10.4$, $\text{SGZ} = -0.4 h^{-1} \text{ Mpc}$.

TABLE 1
MAJOR COMPONENTS OF THE LOCAL SUPERCLUSTER

CLOUD (1)	COORDINATES			DIAMETERS			VOLUME (Mpc ³) (4)	LUMINOUS GALAXIES (5)	GALAXIES PER Mpc ³ (6)	E/S0 CONDENSATIONS (LUM. E/S0 galaxies) (7)	DE VAUCOULEURS GROUPS ASSOCIATED WITH CLOUDS (8)
	SGX (h ⁻¹ Mpc) (2)	SGY (h ⁻¹ Mpc) (3)	SGZ (h ⁻¹ Mpc) (3)	SGX (h ⁻¹ Mpc) (3)	SGY (h ⁻¹ Mpc) (3)	SGZ (h ⁻¹ Mpc) (3)					
10. Virgo Cluster	-2.4	10.4	-0.4	2.2	2.2	2.2 ^a	6	62	10.	entire cluster (34)	18, 19, 25
9. Canes Venatici	4.3	8.8	0.2	14.6	13.6	4.5	470 ^c	87 (99)	0.2	NGC 4274 (3)	LG, 1, 2, 3, 4, 5, 10, 13, 17, 24, 28, 32, 34, 41
8. Virgo II (southern extension)	-6.1	9.9	-0.5	10.6	10.1	3.6	200 ^c	45 (55)	0.3	...	20, 26, 35
7. Leo II	2.5	11.7	-5.6	15.4 × 7.9 ^b			510 ^c	41 (45)	0.1	...	42, 43, 47, 48, 49, 54
6. Virgo III	-7.4	11.9	6.6	11.3 × 5.7 ^b			190 ^c	35 (40)	0.2	NGC 5846 (7)	29, 50
5. Crater (NGC 3672)	-9.3	10.5	-5.0	8.1	6.9	4.0	120 ^c	14 (25)	0.2	...	23, 44
4. Leo I	-0.7	7.3	-2.8	2.6	5.4	3.3	20	15	0.6	M96 (2)	9, 11
3. Leo Minor (NGC 2841)	2.4	4.0	-2.1	7.5	6.6	2.5	60	11	0.2	...	6, 12
2. Draco (NGC 5907)	3.7	6.5	6.0	6.5	2.3	8.1	60	6	0.1	...	30
1. Antlia (NGC 2997)	-4.1	3.3	-5.4	4.5	4.6	3.4	40	5	0.1	...	8
0. NGC 5643	-9.6	3.4	0.8	1	5	1	2	3
Rest of LSC sample	~ 2900 ^d ~ 4500 ^d	8 332	0.003 0.07

Column (1), cloud names. The nomenclature follows de Vaucouleurs 1975*a* whenever possible. Column (2), unweighted cloud center from redshifts and a Hubble constant of $100 h \text{ km s}^{-1} \text{ Mpc}^{-1}$. Column (3), the 2σ cloud dimensions (except Virgo Cluster, see note a). Column (4), the volume of a triaxial spheroid with the dimensions given in col. (3). The volume should contain $\sim 95\%$ of galaxies associated with the cloud. Column (5), the number of galaxies associated with the cloud brighter than $-18 + 5 \log h$ ("luminous galaxies"). Certain clouds extend beyond the boundaries enclosing the "complete" sample. Numbers in parentheses are the *total* number of luminous galaxies associated with individual clouds (see Table 4 in the Appendix). The number of luminous galaxies found within the complete sample boundaries is indicated without parentheses. Column (6), the total number of galaxies associated with the cloud divided by the 2σ volume. Column (7), in addition to the Virgo Cluster, the Local Supercluster contains three small but dense groups containing principally elliptical and lenticular galaxies. These groups are identified, and in parentheses is the number of luminous E and S0 galaxies associated with each group (see Appendix for a discussion). Column (8), the correspondence is given between de Vaucouleurs' 1975*a* groups and the larger scale structure which contains them.

^aGalaxies were assigned to the Virgo Cluster if and only if they are found within 6° of the core of that cluster. At the distance of the Virgo Cluster, 6° corresponds to $1.1 h^{-1} \text{ Mpc}$.

^bThe Leo II and Virgo III clouds are sufficiently skewed from the rectangular supergalactic coordinate system that their dimensions in that system are not very meaningful. It is noted that these structures are approximately prolate and point toward the Virgo Cluster. For each of these two clouds, a coordinate system was established with one axis directed along the line joining the Virgo Cluster and the cloud center. The 2σ dimensions are given for this long axis and the average of the two (randomly oriented) short axes.

^cEach of the noted clouds extends somewhat beyond the boundaries $|\text{SGX}| < 10 h^{-1} \text{ Mpc}$, $|\text{SGY}| < 15 h^{-1} \text{ Mpc}$, $|\text{SGZ}| < 10 h^{-1} \text{ Mpc}$ which contained the "complete" luminous galaxy sample. Total 2σ volumes are given but, between all the clouds, $\sim 100 h^{-3} \text{ Mpc}^3$ lie outside these boundaries.

^dAn attempt has been made to account for the effects of galactic obscuration.

^eThe total number of E and S0 galaxies in the "complete" luminous galaxy sample. Some statistics concerning the distribution of these early morphological types are given in the Appendix.

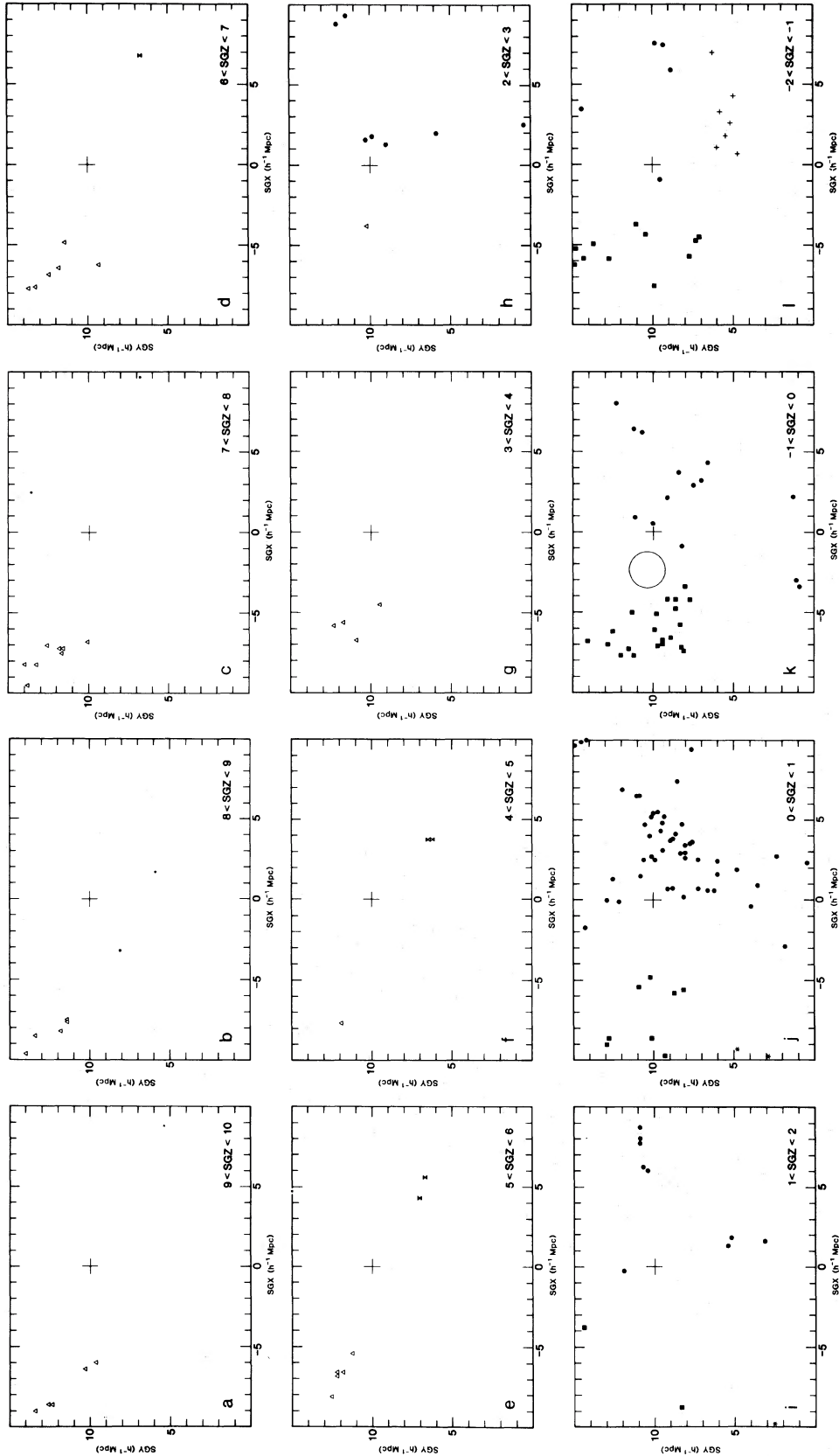


FIG. 6.—The Local Supercluster sliced in thinner sections. The sample of galaxies and the orientation of slices are now only $1 h^{-1}$ Mpc thick, and symbols are now assigned in accordance with proposed cloud memberships. The symbol code is: Canes Venatici (*filled circles*), Virgo III (*filled squares*), Virgo II (*open triangles*), Leo II (*open circles*), Crater (*open squares*), Leo I (*two inverted triangles*), Leo Mi (*pluses*), Antlia (*filled triangles*), Draco (*crosses*), NGC 5643 (*stars*), and unassigned (*small dots*). The Virgo Cluster is located by the ring within the slab: $-1 < \text{SGZ} < 0 h^{-1} \text{ Mpc}$.

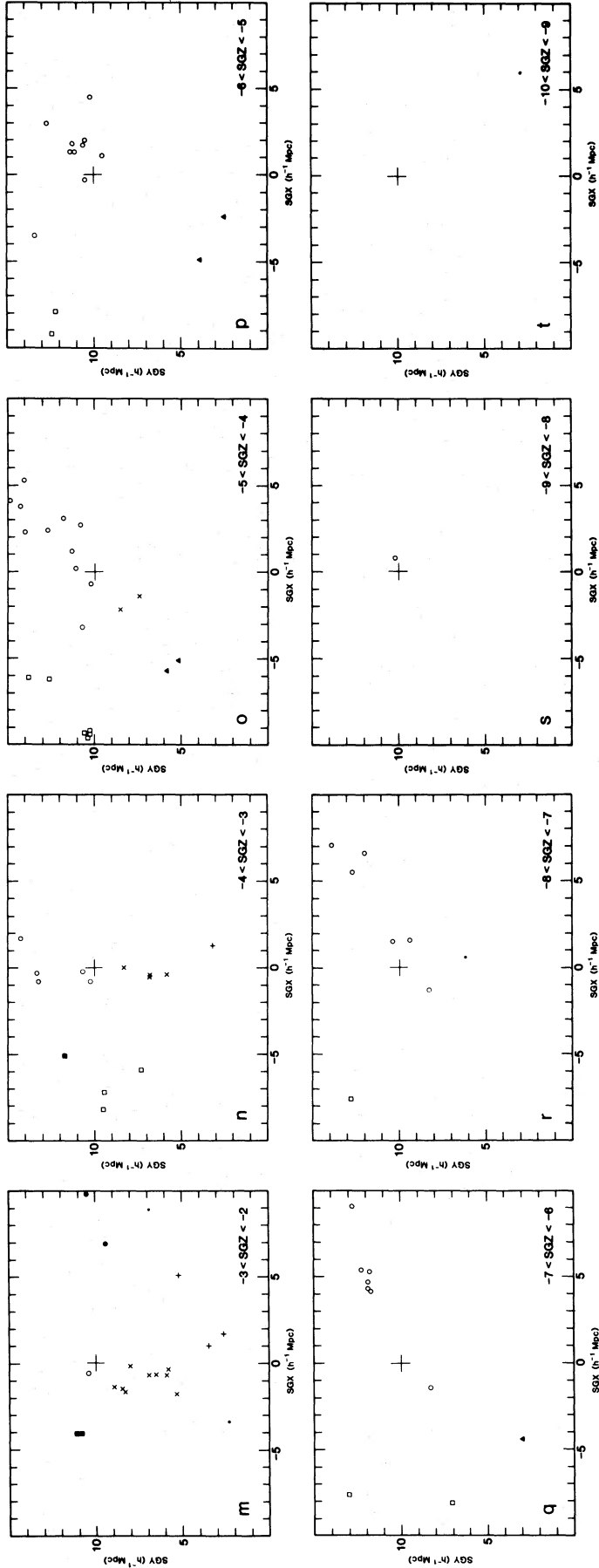


FIG. 6—Continued

tion-free volume above the plane of the supercluster (with a small adjustment per note *c* in Table 1). The 1σ volumes (enclosing two-thirds of the galaxies in the clouds) collectively occupy 30 Mpc^3 , or $\sim 2\%$ of the absorption-free volume.

It can be seen in Figure 7 that there is a distinct minimum in the density of galaxies between both Virgo III and Draco and the clouds defining the flattened plane. It is on this phenomenological basis that these clouds are identified as separate structures.

South of the supercluster plane there is one major cloud, Leo II; three minor clouds, Crater, Leo I, and Leo Minor; and the less important Antlia feature (although the Antlia Cloud is rather rich in low-luminosity systems). In a volume of $\sim 2400 h^{-3} \text{ Mpc}^3$ in the approximate interval $-2 h^{-1} \text{ Mpc} > \text{SGZ} > -10 h^{-1} \text{ Mpc}$ there are again only four galaxies lying outside these five regions. Together, these regions include a 2σ volume of 750 Mpc^3 , or $\sim 42\%$ of the absorption free volume below the supercluster plane (again, see note *c*, Table 1). The 1σ volume of the clouds is 90 Mpc^3 , or $\sim 6\%$ of the total absorption free volume.

In fact, the boundaries between Leo II and Leo I, on the one hand, and Leo I and Leo Minor, on the other, are not without ambiguity, and there will be no effort made to justify detailed membership assignments. The important question is whether it is reasonable to view these structures as distinct from the clouds defining the plane. It has been argued on the basis of the distribution of luminous galaxies on the sky, shown in Figure 7, that the southern clouds *are* isolated. The only ambiguous case is the Leo Minor Cloud because this cloud is the one nearest the supergalactic plane and the statistics are poor. However, our conclusions should not depend on the disposition of 4% of the sample.

In summary, it is argued that the clouds off the plane of the Local Supercluster can be regarded as a separate component from those that constitute the disk because the large majority of luminous galaxies (94%) lying off the supergalactic plane are to be found in only a small number of clouds (7), which occupy a very small fraction of the total volume (2σ shells enclose 30% of the total volume; 1σ shells enclose 4%), and these clouds are each significantly separated from the disk. In particular, it is to be noted that there is no single structure which *bisects* the supercluster plane.

III. A CLOSER LOOK

If the structure in the distribution of nearby galaxies is so extreme, then why has it not been apparent for decades? The answer is that the filling factor of the clouds, while small enough to be interesting, is large enough that any two-dimensional display becomes quite confused as a consequence of projection effects unless the greatest care is taken to isolate components.

Figures 8 and 9 provide an illustration of this point. Between these two figures, we are looking at the projected location on the SGX–SGZ plane of all galaxies in the NBG catalog in a volume only slightly larger than the one discussed in the previous section. (Now, $-14 h^{-1} < \text{SGX} < +13 h^{-1} \text{ Mpc}$, $0 < \text{SGY} < +17 h^{-1} \text{ Mpc}$, $-11 h^{-1} < \text{SGZ} < +11 h^{-1} \text{ Mpc}$.) Galaxies brighter than $-18 + 5 \log h$ (the qualification for membership in the “complete” or “extended” samples) are shown as dots, while less luminous galaxies are represented by crosses in these figures. The distinction between these plots is that Figure 8 includes only those galaxies on the *far* side of this volume, while Figure 9 includes only those galaxies on the *near* side. The separation has been chosen to fall at $\text{SGY} \approx 8 h^{-1} \text{ Mpc}$, although the precise demarcation was gerrymandered so that the Virgo Cluster, Virgo II, Virgo III, Crater, and Leo II would lie in their entirety within the far-side volume, and Leo I, Leo Minor, Antlia, and Draco would be totally within the near-side volume. The Canes Venatici Cloud extends over too large a distance in the radial direction to be conveniently included in only one of these figures, so galaxies in CVn with $\text{SGY} > 8 h^{-1} \text{ Mpc}$ are plotted in Figure 8, and galaxies to the foreground in CVn are plotted in Figure 9.

The perspective shown in Figure 8 was specially chosen because it affords a view of the six most important components of the Local Supercluster clear of projection complications. The six clouds are at roughly the same mean distances, so the ratios of low to high luminosity galaxies (crosses to dots on the figure) are comparable in all of the clouds. With only one exception, there are no additional features revealed by inclusion of the less luminous systems, and they serve simply to add statistical weight to the delineation of structure. The single noteworthy exception is the rather linear alignment of galaxies near $\text{SGX} = +3$, $\text{SGY} = +12$, $\text{SGZ} = +3.5 h^{-1} \text{ Mpc}$. This minor but intriguing feature will be called the Canes Venatici Spur and will receive attention further on in the discussion.

Without any doubt, the most striking aspect of Figure 8 must be the radial elongation of all the clouds with respect to the Virgo Cluster—like spokes on a cartwheel. It is to be recalled that this view is affected very little by the velocity component to positions. The spokes are to be seen in Figure 7*b* if one mentally filters out the foreground clouds.

We will take a closer look at the elongated form of clouds near the Virgo Cluster, but first we turn our attention to Figure 9. All the clouds featured in this volume are quite nearby, so the ratios of low-luminosity to high-luminosity systems are much larger than in the clouds of Figure 8. Consequently, we get a biased impression of the relative significance of these nearby clouds. However, this figure serves two disparate purposes: (i) Superposition of Figures 8 and 9 illustrates the

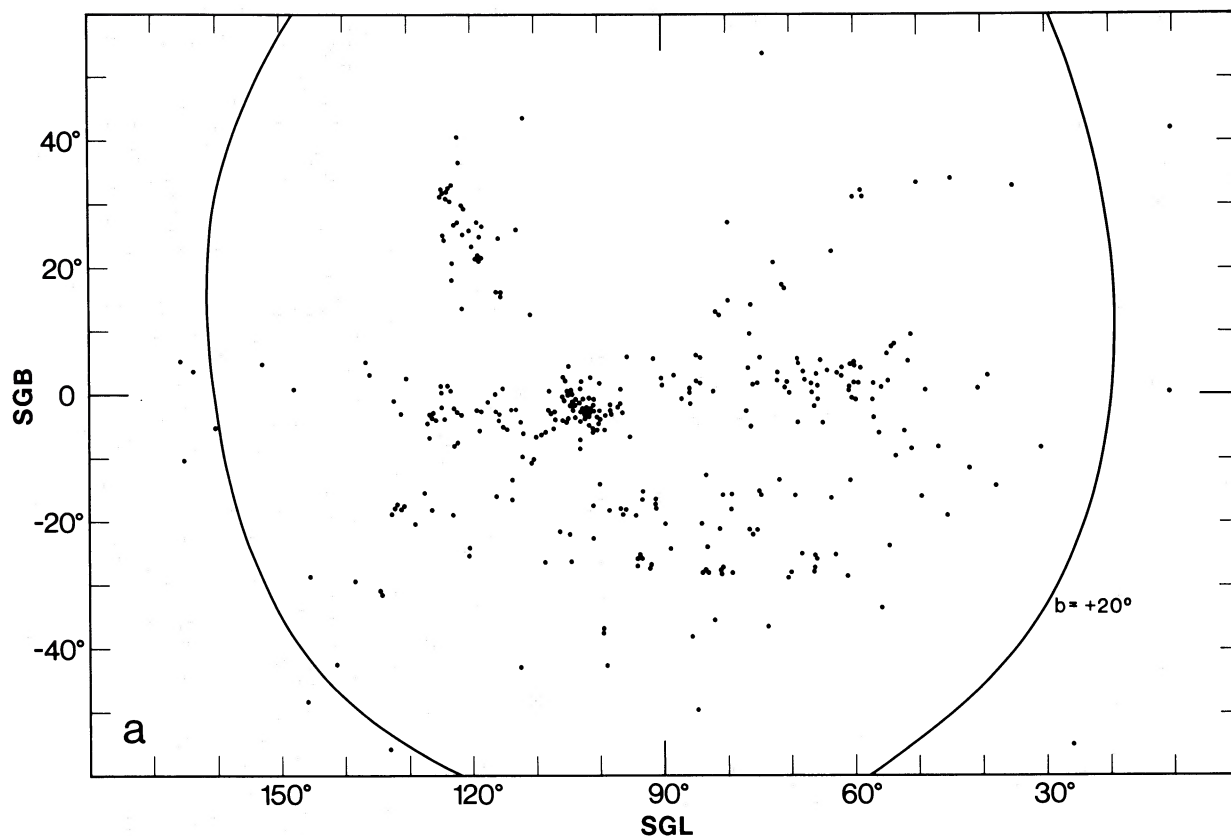


FIG. 7a

FIG. 7.—(a) The distribution on the sky of the “complete” and “extended” samples of galaxies. The zone of avoidance ($b < 20^\circ$) is indicated. (b) Cloud assignments for the galaxies plotted in Fig. 7a. The symbol code is the same as in Fig. 6, except that now small dots serve double duty, identifying galaxies in the Virgo Cluster as well as unassigned galaxies.

difficulties caused by projection effects. (ii) We must be struck by the *emptiness* of the upper-left quadrant.

Rather than plotting the projected distribution of individual galaxies as was done in Figure 8 and 9, it is useful for the delineation of individual clouds to blur the data and plot surface density contour maps. Figure 10a is such a smoothed version of Figure 8. The smoothing function is a Gaussian with a sigma of $0.5 h^{-1}$ Mpc. Figure 10b is a smoothed version of the distribution of *luminous* galaxies in Figure 8 (i.e., the dots only).

To proceed further, the individual clouds must be isolated. The volume enclosing the supercluster will be partitioned in a way that one and only one cloud is contained within a given partition volume. Then each such region will be displayed from the three cardinal directions in Cartesian supergalactic coordinates. Contour maps analogous to those in Figure 10 will be shown, but with the smoothing function reduced to $\sigma = 0.25 h^{-1}$ Mpc. On occasion, the volumes had to be partitioned in an irregular way to maintain the separa-

tion of the principal clouds. All galaxies in Figures 8 and 9 appear in one and only one partitioned volume, with the following exceptions. Galaxies associated with the 6° radius Virgo Cluster have been excluded from all maps. The foreground region $SGX < -2$, $SGZ > -1 h^{-1}$ Mpc is not contained in any subsequent map. This region includes the very minor NGC 5643 Group, the nearby Centaurus Group which is taken to be part of the CVn Cloud, and the great empty zone seen in Figure 9. The CVn Spur extends from near the supercluster plane in Canes Venatici to the background of Draco. Galaxies in this feature each fall in two maps: once in the maps isolating the spur and again in either the Canes Venatici or Draco maps.

Since, except in Canes Venatici, the galaxies in the individual clouds are roughly at a common distance, there will be little differential in the ratio of faint to bright galaxies across a given cloud. Consequently, all galaxies at our disposition will generally be used to delineate the individual clouds. Some of the nearest

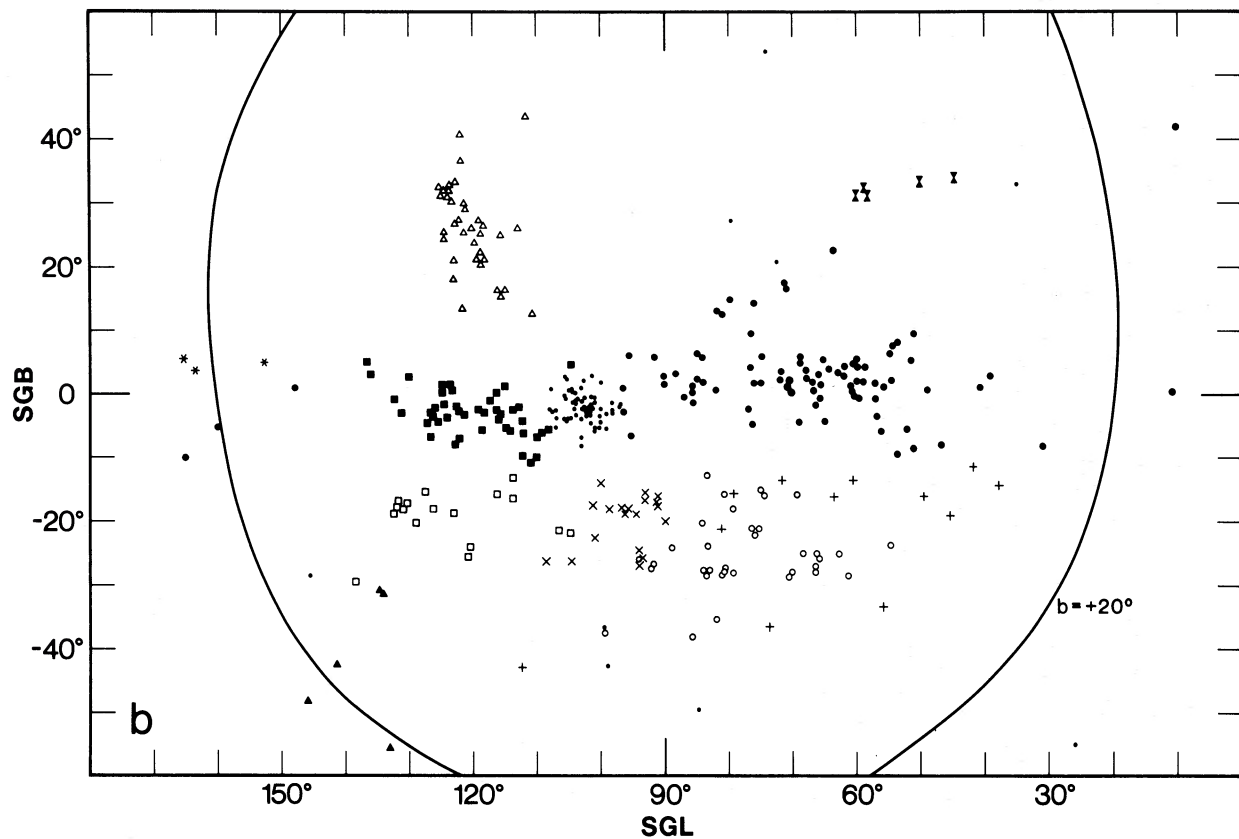


FIG. 7b

clouds, like Leo Minor, have few bright members but can be studied in some detail thanks to the large number of low luminosity systems that are associated.

The two clouds which define the plane of the Local Supercluster are mapped in Figures 11 and 12 (Canes Venatici) and in Figure 13 (Virgo II). All galaxies in the CVn region are plotted in Figure 11, while only those more luminous than $-18 + 5 \log h$ are plotted in Figure 12. The important point that these maps emphasize is that both CVn and Virgo II are crudely *oblate* structures.

The Virgo III and Leo II regions are shown together in Figure 14, and the Crater and CVn Spur regions are shown together in Figure 15. These particular pairs can be displayed jointly because they do not overlap in any of the three orthogonal projections. However, the larger purpose with these paired displays is to determine if the suggestive symmetry of these features on each side of the Virgo Cluster seen on the SGY-SGZ projections of Figures 8 and 10 is seen in the other two projections.

My tentative conclusion is that the symmetry seen in SGX-SGZ projections is fortuitous. For Virgo III and Leo II, the symmetry is broken in the SGX-SGY and

SGY-SGZ projections (Fig. 14). Both these clouds appear to be beyond Virgo. Velocity effects are important parallel to the SGY axis. However, estimates of distances to these clouds independent of redshift appear to confirm the proposition that both of these clouds are slightly farther away than the Virgo Cluster.

It can be firmly concluded that Virgo III and Leo II, and argued that Crater and the CVn Spur, are all crudely *prolate structures pointed with their long axes toward the Virgo Cluster*. It is in the SGX-SGY and SGY-SGZ projections of Figure 14 that one sees most clearly that the elongations are, indeed, toward the Virgo Cluster. It might be feared that velocity effects place this conclusion in jeopardy. However, velocity effects will tend to distend the apparent structure in the direction toward the Earth, not toward Virgo (the finger of God, pointing out our mistake). There is the obvious possibility that galaxies nearest Virgo will have larger infall motions than galaxies farther away. Such motions would be seen by us as relative blueshifts in clouds beyond Virgo and relative redshifts in clouds on the near side of Virgo. The expectation would be that, in clouds just beyond Virgo, those galaxies nearest Virgo

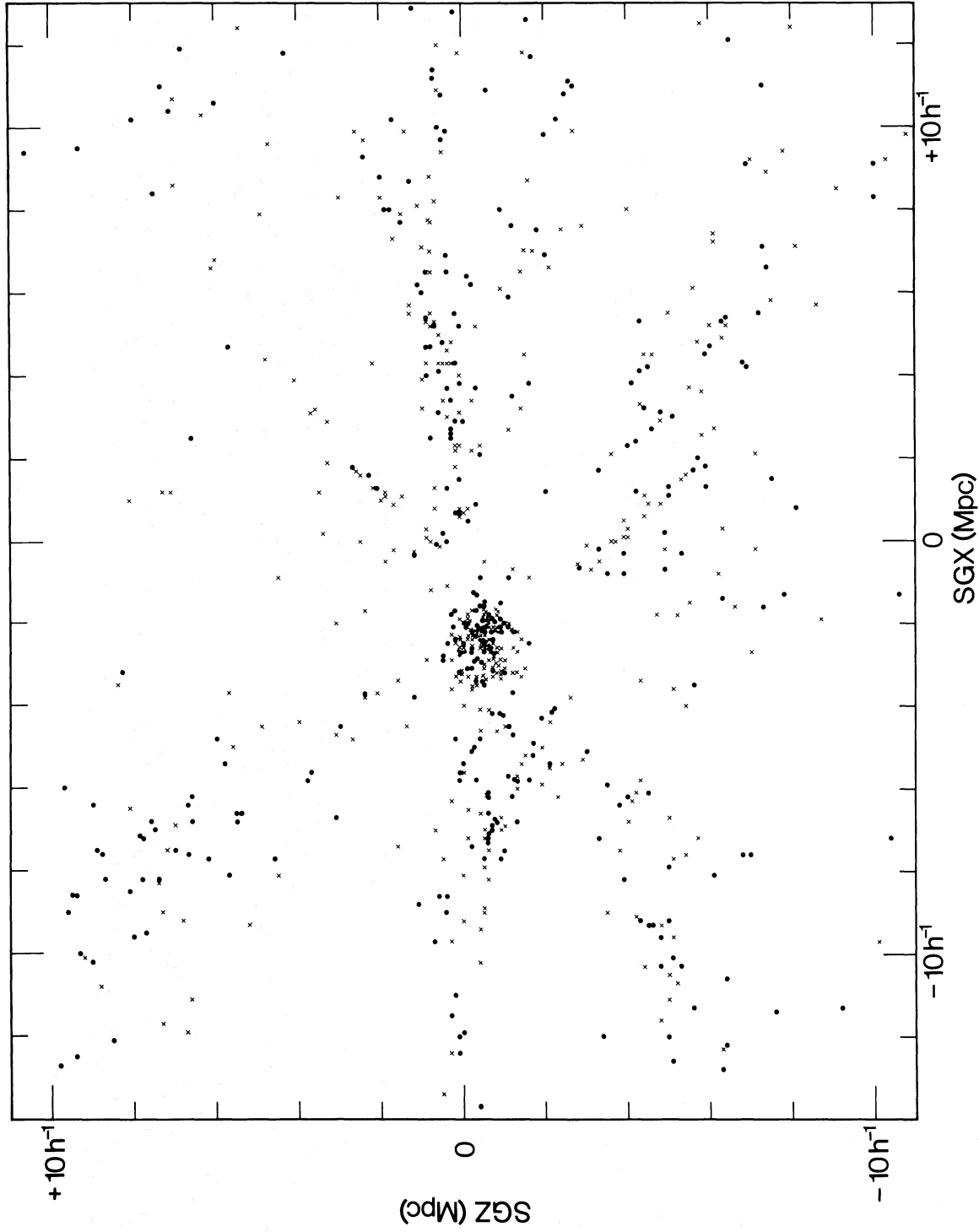


FIG. 8.—The distribution of 672 galaxies in the vicinity of the Virgo Cluster, projected onto the SGX-SGZ plane. Filled circles indicate galaxies brighter than $-18 + 5 \log h$, and crosses indicate galaxies fainter than this limit. The volume extends in depth to $SGY \approx +17 h^{-1}$ Mpc. The foreground limit is at approximately $SGY \sim +8 h^{-1}$ Mpc, but was defined in an irregular way so that the foreground clouds Leo I, Leo MI, Antlia, and Draco would be entirely excluded, and the more distant clouds Virgo, Virgo II, Virgo III, Leo II, and Crater would be entirely included. Only the distant half of Canes Venatici is included.

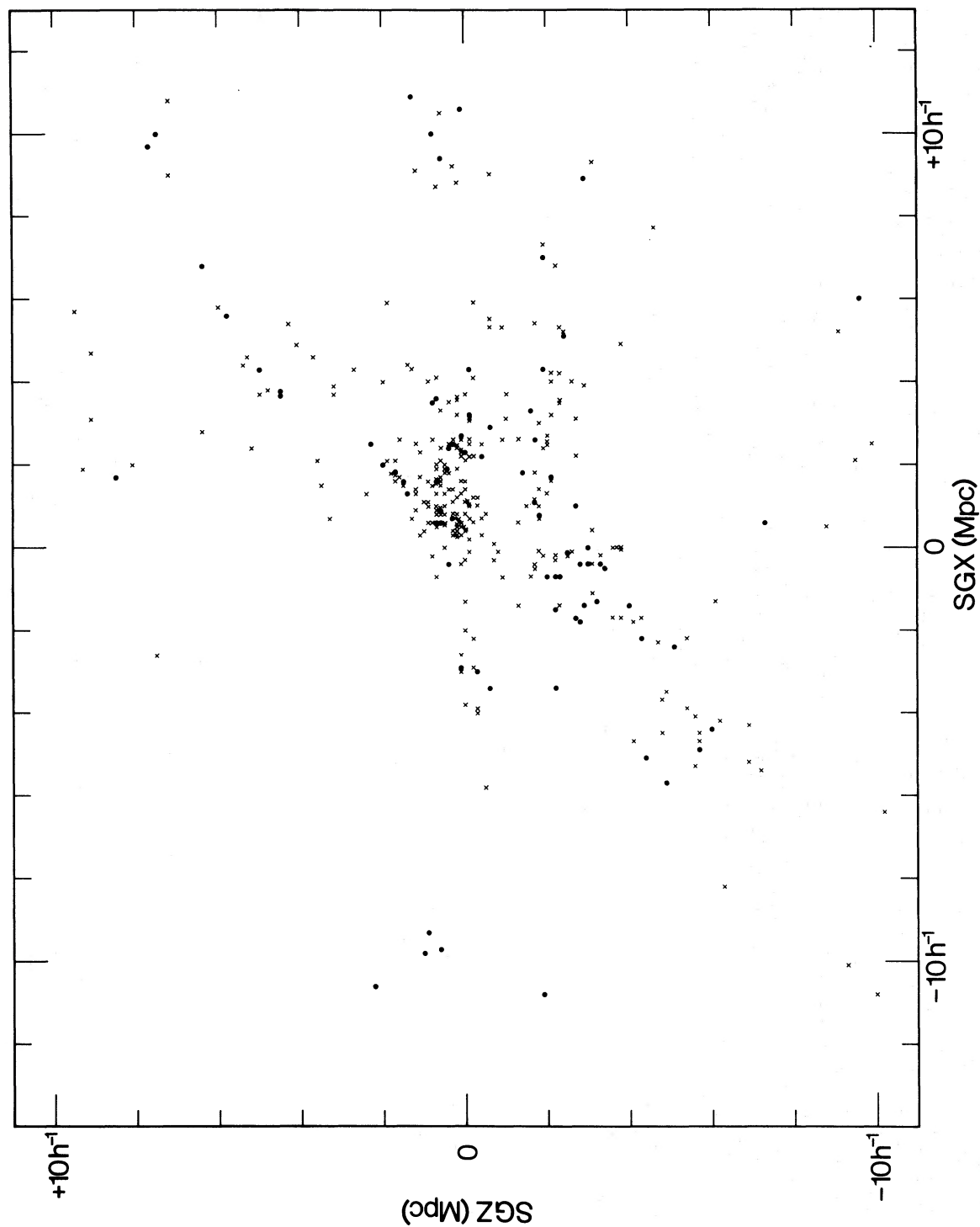


FIG. 9.— The distribution of 350 nearby galaxies projected onto the SGX-SGZ plane. The symbols are defined the same as in Fig. 8. The volume extends from $SGY = 0$ to the foreground limit of Fig. 8 at $SGY \sim 8 h^{-1}$ Mpc. This volume includes the clouds Leo I, Leo Mi, Antlia, Draco, the NGC 5643 Group, and the foreground half of Canes Venatici.

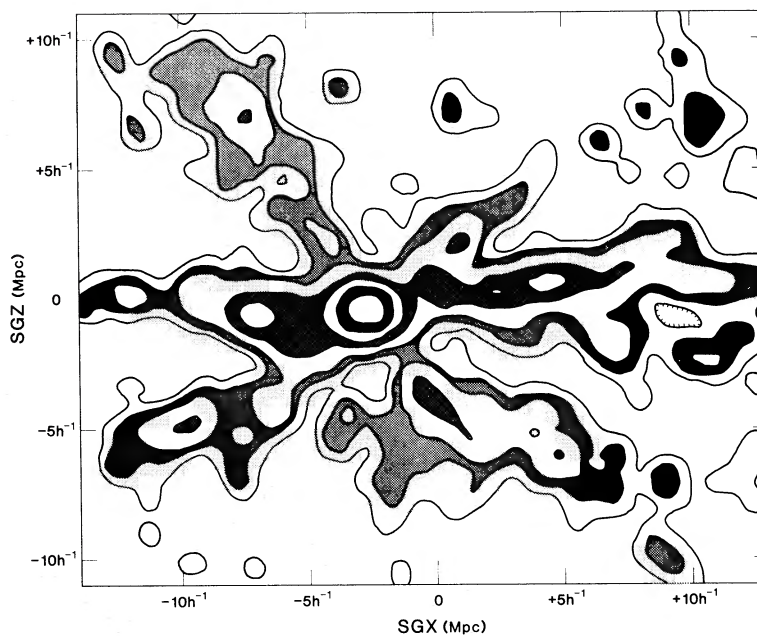


FIG. 10a

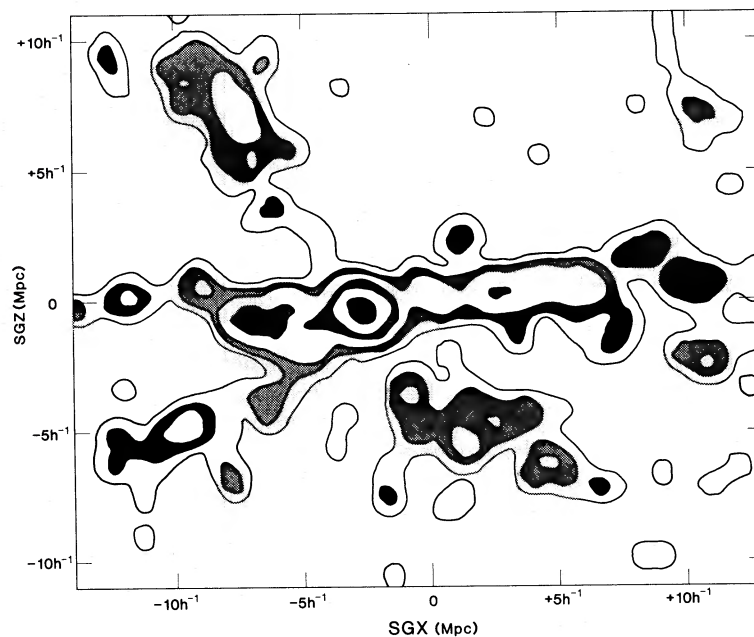


FIG. 10b

FIG. 10.—(a) Contour map of the distribution of *all* NBG galaxies near the Virgo Cluster projected onto the SGX–SGZ plane. This figure is an alternative display of the distribution of the galaxies in Fig. 8. Surface densities have been computed by smoothing with a Gaussian with $\sigma = 0.5 h^{-1}$ Mpc. Contours are on a *logarithmic* scale. The lowest contour corresponds to surface densities of $0.5 \text{ galaxies Mpc}^{-3}$. Successive contours correspond to levels of 1, 2, 4, 8, 16, and 32 galaxies Mpc^{-3} . (b) The same display as Fig. 10a but for *luminous* galaxies only. The surface density of those galaxies plotted as filled circles in Fig. 8 is shown. The smoothing function and contour levels are the same as in Fig. 10a.

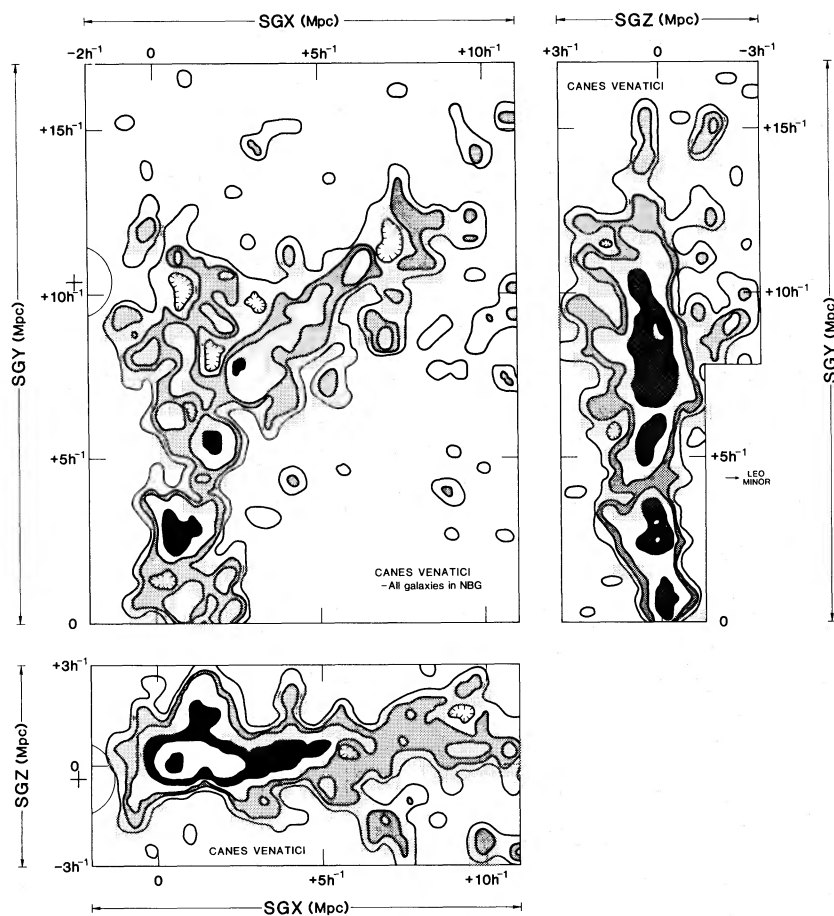


FIG. 11.—The Canes Venatici Cloud including all 327 galaxies in the NBG catalog located within the volume defined by the outer rectangular boundaries. The projection onto the SGX–SGY plane is given in the upper left panel, the SGY–SGZ projection is given in the upper right panel, and the SGX–SGZ projection is given in the lower left panel. Surface densities are computed with a smoothing function with $\sigma = 0.25 h^{-1} \text{ Mpc}$. Contour levels are 1.5, 3, 6, 12, 24, and 48 galaxies Mpc^{-3} . This cloud is the largest one in the Local Supercluster, and together with Virgo II, defines the plane. Because this cloud, in which we reside, has such a great extent in the line of sight, the foreground part is dramatically overemphasized by the inclusion of low luminosity systems. This figure should be compared with Fig. 12 which illustrates the distribution of the intrinsically luminous galaxies only. The Canes Venatici Cloud actually extends slightly into the south galactic hemisphere ($\text{SGY} < 0$). The location of the Virgo Cluster is indicated by the large crosses.

would erroneously be placed to the foreground of their true position. We are very likely observing such an effect in the CVn Spur, and possibly in both Virgo III and Leo II. However, the fact that in each case the apparent elongation is at most only mildly perturbed from alignment with Virgo *in spite of* kinematic effects is convincing evidence that the fingers can be attributed not to God but to Newton.

It has been remarked that there is good correspondence between the distribution of faint galaxies and the distribution of luminous galaxies, with the CVn Spur being the most notable exception that has so far been discussed. This feature is very close to the Virgo Cluster in projection. If it is located slightly *beyond* Virgo and has a substantial infall velocity toward Virgo, then the assumption of a uniform Hubble flow would have led to

the underestimation of the luminosities of galaxies in this region. The reasonableness of this interpretation alerts us to a real problem. Factor of 2 departures from uniform expansion can certainly be anticipated in the region of the Virgo Cluster, with corresponding 1.5 mag fluctuations in the level of the luminosity function of galaxies to which we are sampling if we work to a magnitude limit. In fact, there seem to be only two regions other than the CVn Spur where there are quite substantial streaming motions affecting our observations in the manner that has just been described. Within the Canes Venatici Cloud, there are a small number of galaxies in the vicinity of NGC 4565 which are probably on the *near* side of the Virgo Cluster and falling away from us. The more important and certain case is the rather rich group in the vicinity of NGC 4636 and NGC

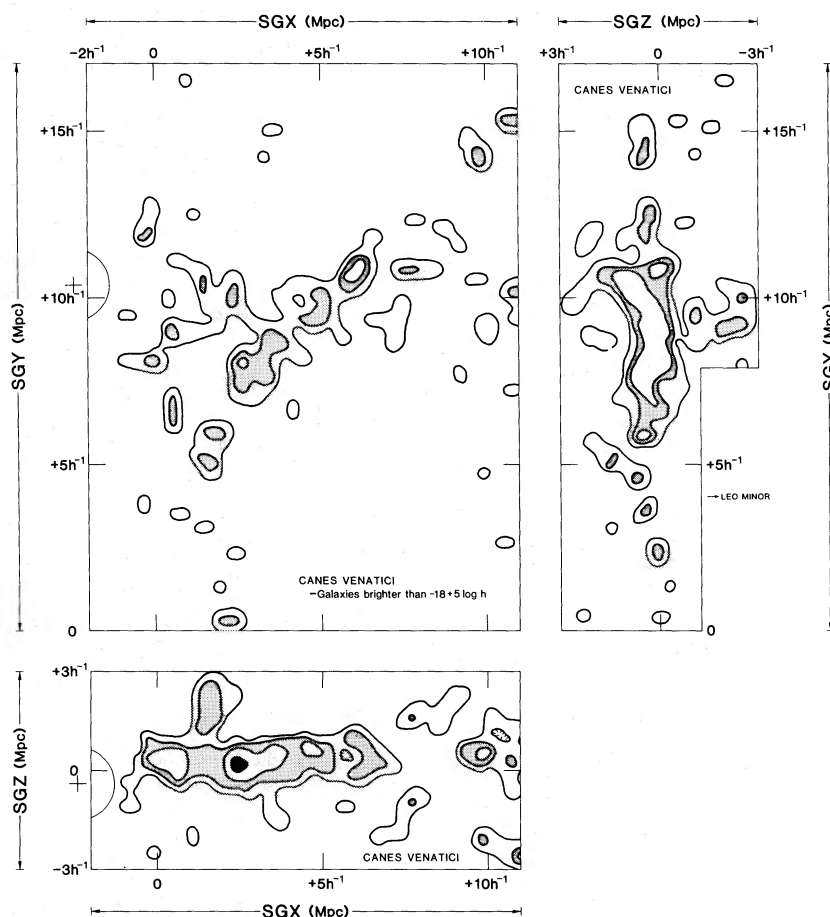


FIG. 12.—The Canes Venatici Cloud including only 96 galaxies more luminous than $-18+5 \log h$. The smoothing and contour levels are the same as in Fig. 11. This display is not biased in favor of the foreground as was Fig. 11.

4665, within the Virgo II cloud (at $SGX = -2.5$, $SGY = +6$, $SGZ = 0 h^{-1}$ Mpc). Distances have been determined to several galaxies in that group using the H I profile-magnitude relationship (Tully and Fisher 1977), and it is found that this group is slightly beyond Virgo, although all members of the group are *blueshifted* with respect to the Virgo Cluster barycentric velocity. The projected motions of galaxies in this group toward Virgo can be as large as 500 km s^{-1} . This group is destined to be digested into the Virgo Cluster.

The less important foreground clouds are displayed in Figures 16 (Leo I), 17 (Leo Mi),⁴ and 18 (Antlia). Leo Minor turns out to be a rather substantial complex when low-luminosity systems are retained. The surprise is that this cloud, like CVn and Virgo II, can be described as *oblate*, and its principal plane lies parallel to the main plane of the supercluster. The separation between these two planes is only $2 h^{-1}$ Mpc (if redshift-independent

⁴In fact, the separation between Leo I and Leo Mi is ambiguous, and a description of this region in terms of a single cloud might be warranted.

distances are used the separation turns out to be greater). This structure may not be unique. In Figures 8, 10, and 11 (lower left panel) it can be seen that the Canes Venatici Cloud appears to bifurcate. The segment in the vicinity of $7 < SGX < 11$, $SGY \approx 9$, $SGZ \approx -2 h^{-1}$ Mpc could easily be a more distant analog of the Leo Mi Cloud.

Finally, a very large volume of space above the galactic plane is displayed in Figure 19. The region contains the Draco Cloud in the foreground and the CVn Spur in the background.

IV. WHAT CAN IT ALL MEAN?

a) *The Structure off the Plane*

From the dimensions of the clouds given in Table 1 and from the contour maps, it can be seen that in a crude sense the clouds *off* the supergalactic plane (save Leo Mi) can be described as being *prolate*. There is substantial evidence that at least the most important clouds—Virgo III, Leo II, and probably Crater—are

TULLY

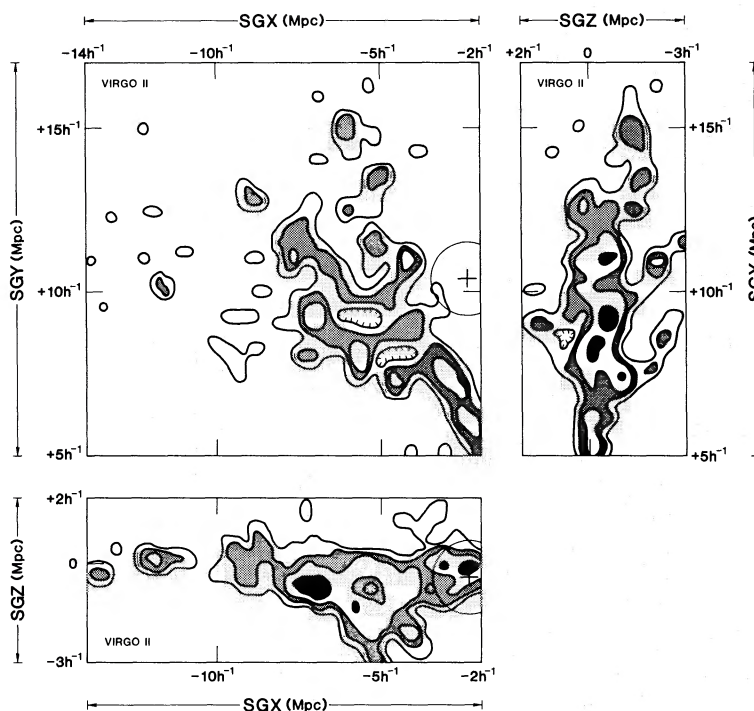


FIG. 13.—The Virgo II Cloud (the Virgo southern extension). These maps display the distribution of 122 galaxies in the other of the two major clouds which define the plane of the Local Supercluster. The galaxies nearest to the Virgo Cluster in projection, and probably in space, are located within this cloud. The projection, smoothing, and contour values are the same as in Fig. 11. Galaxies associated with the 6° Virgo Cluster have been excluded, but the location of this cluster is indicated on each map.

directed such that their respective long axes *point toward the Virgo Cluster*. The obvious interpretation of these observations is that the elongated structures are the consequence of tidal action which began at an earlier epoch when the clouds were closer to the Virgo Cluster (Binney and Silk 1979).

A detailed consideration of this problem would represent too great a distraction from the thrust of the present discussion. The matter will be given brief attention here. A more extensive analysis will be published by Shaya and Tully (in preparation).

We can attempt to specify the era when tidal forces would have been important following the spirit of the analysis presented by Hartwick (1976). Shaya has pointed out that a specific deficiency in the discussion by Hartwick, which propagated through the ensuing discussion by Tully (1980), was a failure to account for a look-back effect, given that the perturbing potential causing tidal effects arises out of the *overdensity* of the perturber region compared with the mean density of the universe. The density contrast of the Virgo region today may be sufficiently high that subtraction of the mean density is a minor effect, but this contrast was considerably reduced in the past.

If a perturbed cloud is at a distance R from the center of a spherically symmetric overdense region in which the

density falls off as $R^{-\gamma}$, then the usual Roche criterion can be written

$$r_t = \left(\frac{3}{2\gamma} \frac{m}{\delta M} \right)^{1/3} R, \quad (1)$$

where r_t is the tidal radius in a cloud of mass m , and δM is the excess mass within a volume of radius R that is the cause of the disruption.

If it is assumed that the perturbing and perturbed masses are freely separating in an Einstein-de Sitter universe and, further, that the density contrast of the perturber has been growing only linearly (recall that the perturbing region is a much larger volume than simply the Virgo Cluster), then the time dependence of the density enhancement is of the form

$$\frac{\delta M}{R^3} \sim \bar{\rho} \delta \sim t^{-2} t^{2/3} \sim t^{-4/3}, \quad (2)$$

where the mean density in the universe is $\bar{\rho}(t)$, and the density contrast under consideration is $\delta(t) = \delta\rho/\bar{\rho}$. Given the relationship between redshift and the age of the universe (where $z = 0$ at $t = t_0$),

$$1 + z = (t_0/t)^{2/3},$$

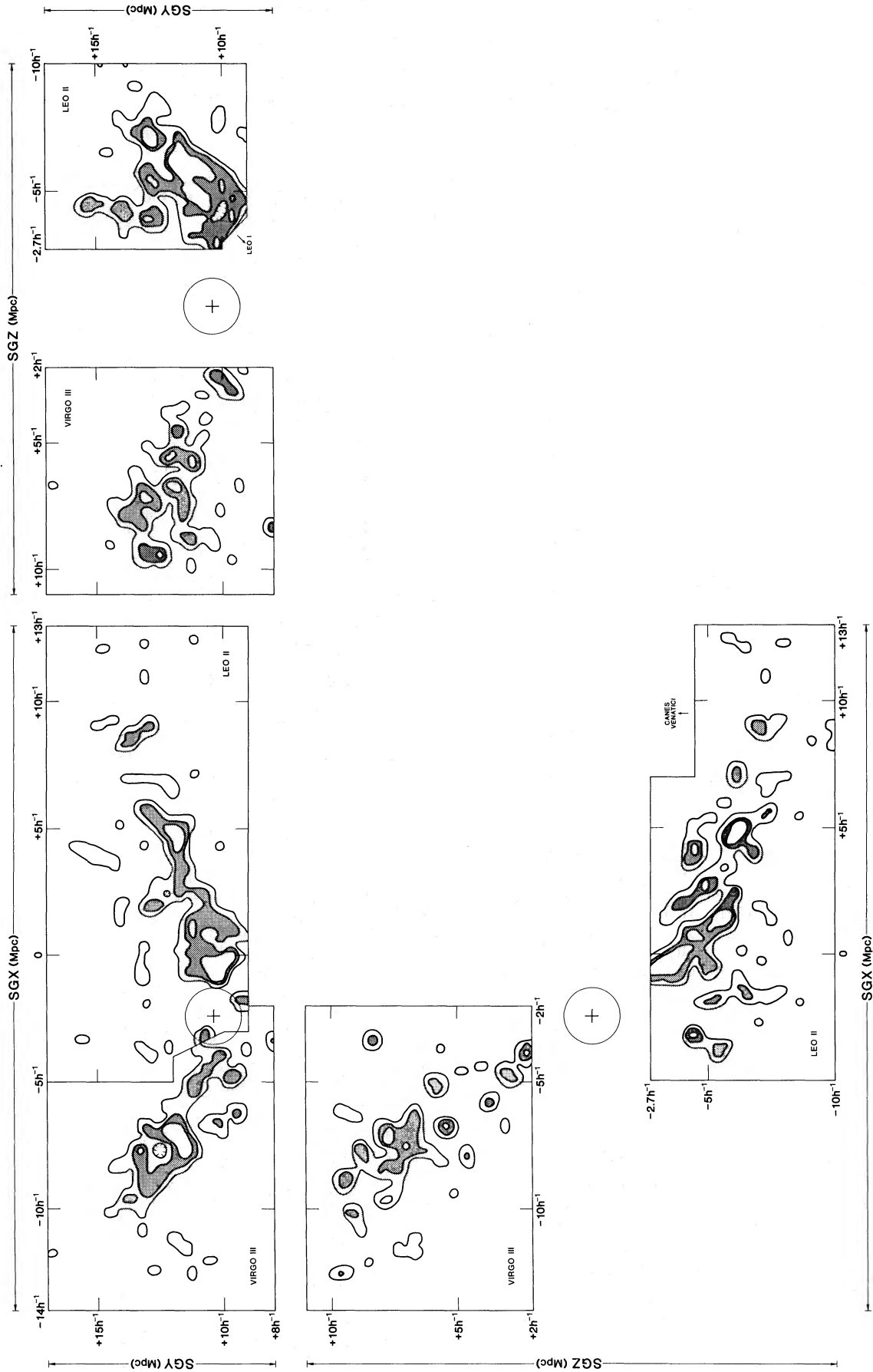


FIG. 14.— The Virgo III and Leo II clouds. These maps illustrate the structure within the two most important clouds off the plane of the supercluster. There are 62 galaxies in the Virgo III region and 102 galaxies in the Leo II region. The position of the Virgo Cluster is indicated by the cross and 6° radius circle. It is evident that the clouds are elongated toward the Virgo Cluster, rather than toward us at $(0,0,0)$. For the Leo II Cloud it is the SGX-SGY projection which offers the clearest proof of this statement, and for the Virgo III Cloud it is the SGY-SGZ projection which is the most convincing.

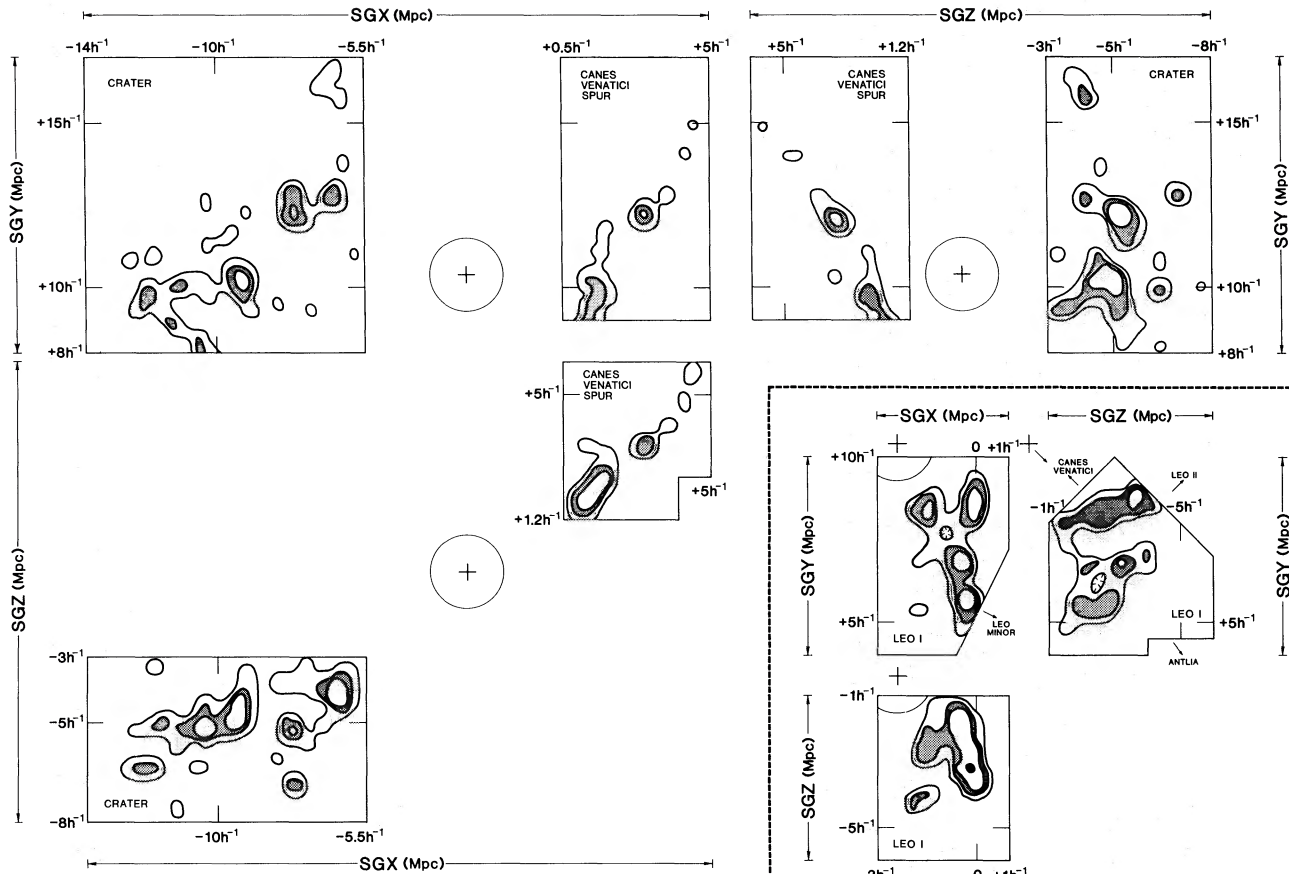


FIG. 15

FIG. 16

FIG. 15(*left*).—The Crater Cloud and the Canes Venatici Spur. These maps illustrate the other important features in close proximity to the Virgo Cluster off the supergalactic plane. There are 45 galaxies associated with the Crater region and 19 with the Spur. The projections, smoothing, and contour levels are the same as in Fig. 11. The maps of the CVn Spur isolate a small region which is also contained, in part, in the Canes Venatici Cloud maps (Fig. 11) and, in part, in the Draco Cloud maps (Fig. 19).

FIG. 16(*bottom right inset*).—The Leo I Cloud. This cloud of 30 galaxies includes the nearest compact group of predominantly early systems, the M96 Group. The Leo I and Leo Mi clouds (Fig. 17) are quite close and the distinction between them may not be justified. Formally, galaxies in the region with $SGY > 2 SGX + 5.2 h^{-1} \text{ Mpc}$ were assigned to Leo I.

then it follows that

$$1 + z = \left[\frac{3}{2\gamma} \frac{m}{\delta M_0} \left(\frac{R_0}{r_t} \right)^3 \right]^{1/2}. \quad (3)$$

The subscript zero implies the present epoch.

There is the prospect that all the parameters on the right-hand side of equation (3) can be deduced from observations and, consequently, that the epoch of tidal disruption can be determined. The most difficult parameter to define from the observations is r_t , the purported tidal radius. It could be that the distorted clouds have been expanding and that observed dimensions within

the cloud must be carried back in time. Fortunately, there is a *condensation* within the Virgo III Cloud, the NGC 5846 Group (de Vaucouleurs group 50), that is surely bound and probably virialized. It is possible to establish an *upper limit* for the redshift of the collapse of this entity.

We tentatively identify 10 galaxies with the NGC 5846 Group. Eight of these are either elliptical or lenticular systems, and eight are brighter than $-18 + 5 \log h$. The unweighted velocity dispersion of the group is $v_p = 254 \text{ km s}^{-1}$. The unweighted inertial radius (Jackson 1975) is $r_t = 295 h^{-1} \text{ kpc}$, and the unweighted rms radius is $r_o = 313 h^{-1} \text{ kpc}$. The crossing time for the

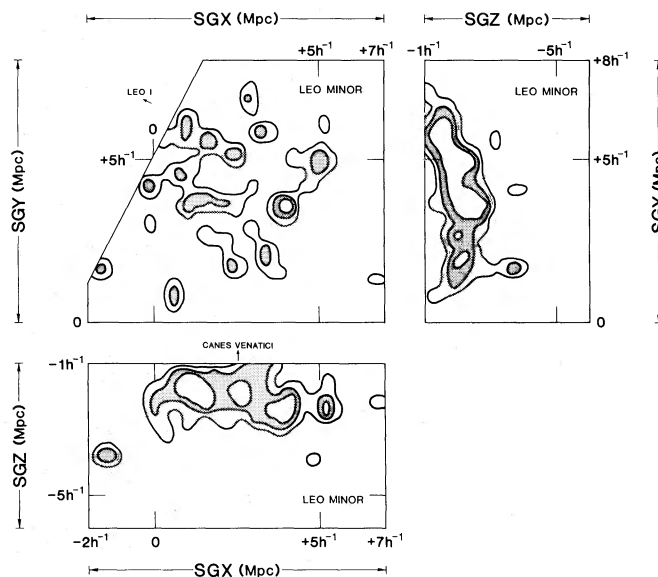


FIG. 17.—The Leo Minor Cloud. There are 47 galaxies known in the region of this cloud, which is the nearest one beyond our own. This cloud is quite close to both Leo I and Canes Venatici, and if it were located two or three times further away it may not have been identified as a separate feature. Like Antlia and CVn, this cloud may extend into the zone of avoidance.

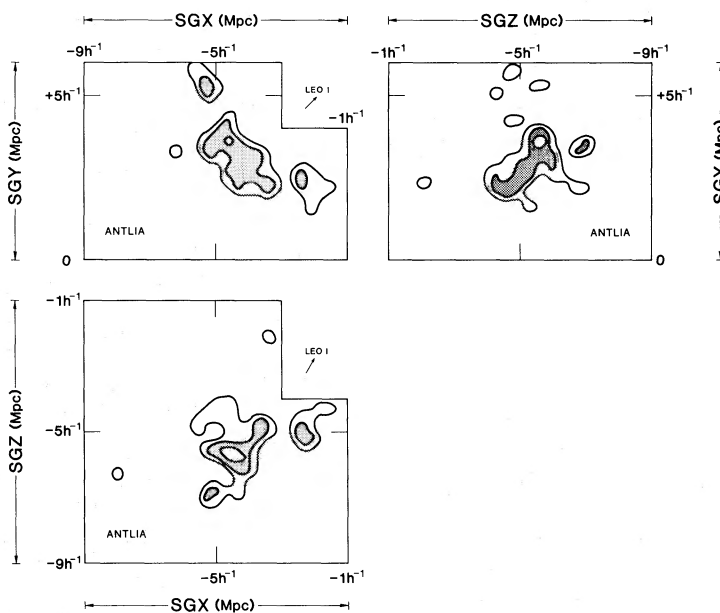


FIG. 18.—The Antlia Cloud. This small cloud, which includes 22 galaxies, is sufficiently isolated and nearby that it can be unambiguously identified as a separate feature. As can be seen in Fig. 7, this cloud lies near the galactic plane so our view of it may be incomplete.

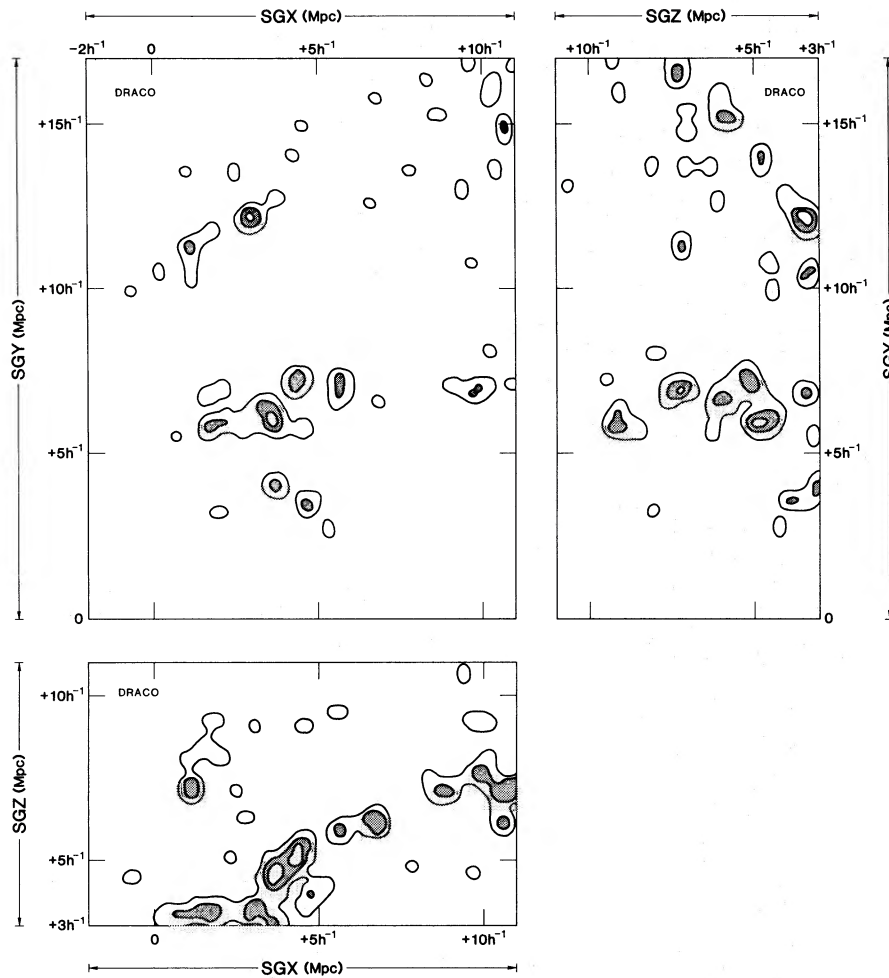


FIG. 19.—The Draco Cloud and beyond. These maps display the distribution of 59 galaxies in a volume of $1800 h^{-3} \text{ Mpc}^3$ north of the plane of the supercluster. The only prominent features are the Draco Cloud at $\text{SGY} \sim 6 h^{-1} \text{ Mpc}$ and part of the CVn Spur at $\text{SGY} \sim 12 h^{-1} \text{ Mpc}$.

group in units of the Hubble time is

$$T_I H_0 = \frac{(3/2)^{1/2} r_I H_0}{3^{1/2} v_p} = 0.08,$$

where the coefficients account for the statistical effects of projection. With such a short crossing time the group must be bound. The ratio $v_p/r_I H_0 = 9$ suggests that the group is virialized.

The existence of this group puts a limit on the effects of tidal stresses. The group was most vulnerable at the epoch of maximum expansion. If it is assumed that the group collapsed spherically and without dissipation, then the dimensions of the group at that epoch were roughly twice the presently observed dimensions. Corrected for projection effects, the present unweighted rms radius is $400 h^{-1} \text{ kpc}$, so for the survival of the group at the

moment of maximum expansion, $r_t > 0.8 h^{-1} \text{ Mpc}$. If the assumptions about sphericity or dissipation are erroneous, it is likely that the dimensions of the cloud would once have been greater, the limit on r_t would increase, and the limit on the redshift would decrease.

There are uncertainties enough in the other parameters required to solve equation (3). The distance of the NGC 5846 Group from the center of the Virgo Cluster is $R_0 = 11 h^{-1} \text{ Mpc}$, assuming no perturbations to a uniform Hubble expansion. Based on the information given in § Va and on the assumption that the mass in the supercluster is distributed in a manner similar to the luminous galaxies, then $\gamma = 2$. For the moment it will be accepted that

$$m/\delta M_0 = N_c / (N_V - \bar{N}),$$

where $N_c = 8$ is the number of luminous galaxies associ-

ated with the NGC 5846 Group, $N_v = 341$ is the number of luminous galaxies in a sphere of radius R_0 centered on the Virgo Cluster (of course it would be more appropriate to consider a flattened spheroid), and $\bar{N} = 103$ is the expected number of luminous galaxies within the volume bounded by R_0 if the region had the mean density of the universe.

This latter number is especially poorly known. The estimate that is given was derived by accepting the mean luminous density quoted by Davis and Huchra (1982) of $1.2 \times 10^8 h L_\odot \text{ Mpc}^{-3}$ (with a 10% correction to the system of luminosities employed in this paper) and the Schechter (1976) luminosity function. A check is provided by comparison with the density of nearby luminous galaxies in the *south* galactic hemisphere. There are 178 galaxies brighter than $-18 + 5 \log h$ with $v_0 < 2000 \text{ km s}^{-1}$ and $b < -30^\circ$. If this volume, which includes both the Fornax Supercluster and some large empty areas, is taken as representative of the mean density of the universe, then $\bar{N} = 118$ is expected in the Virgo perturber region. The two estimates of \bar{N} are in fortuitously good agreement. The Davis and Huchra (1982) value is preferred because it is derived from observations of a larger volume. It is assumed that this volume represents a fair sample of the universe. Of course, accepting that the relative perturber and perturbed masses are given by the luminous galaxy counts presumes common mass-to-light values for these entities.

After only 14 assumptions, we conclude that the epoch of maximum expansion of the NGC 5846 Group within Virgo III was no farther back in time than the corresponding redshift $z \sim 8$.

Condensed groups of a similar nature do not exist in the Leo II Cloud. There are several apparent loose groups in Leo II and Virgo III, but it is not straightforward to prove that they are bound. This discussion will not be continued further in this paper, but it is evident that the subject of the timing of tidal effects on structure on scales of the supercluster deserves serious study.

b) The Structure in the Plane

Some 60% of the luminous galaxies associated with the Local Supercluster are narrowly confined to a thin plane. Two-thirds of these galaxies are outside of the Virgo Cluster. Two extended clouds were identified; but whatever the merit of this separation, these crudely oblate structures together define a common plane. Our own Galaxy lies within the Canes Venatici Cloud. Some characteristics of the supercluster plane are summarized in Table 2.

Several points can be made. In the first place, the two extended clouds taken together are flattened in the ratio SGX:SGY:SGZ/6:3:1. It is important to note that dimensions parallel to the SGZ axis are almost indepen-

TABLE 2
PROPERTIES OF THE SUPERCLUSTER PLANE

Components.....	CVn and Vir II clouds
No. of galaxies	
($M_B^{b,i} < -18 + 5 \log h$).....	154
Unweighted centroid (h^{-1} Mpc):	
SGX.....	0.3
SGY.....	9.6
SGZ.....	-0.1
Rms dimensions (h^{-1} Mpc):	
SGX.....	± 6.3
SGY.....	± 3.2
SGZ.....	± 1.1

dent of line-of-sight effects, and dimensions parallel to SGX are largely so. Velocities have a strong affect on the SGY component, but the dimension along this axis is of intermediate value. Consequently there can be confidence that the ratio of the long and short axes is at least *six to one*. This claim is *not* sensitive to velocity effects. If Galactic absorption plays a role, it could only be *truncating* dimensions ascribed to the *long* axis.

Perhaps more interesting than the relative axial ratios is the *absolute value* of the dispersion in the SGZ direction: $\sigma_z = \pm 1.1 h^{-1} \text{ Mpc}$. If the disk was formed infinitely thin and subsequently has been expanding freely, then the clouds would have puffed to their observed thickness in a Hubble time if rms random motions were only 100 km s^{-1} . These numbers are conservative in the sense that they are derived from the global SGZ distribution of galaxies associated with the disk. It can be seen in Figure 8 that the disk is actually corrugated and bifurcated. The *local* distribution of galaxies normal to the plane is only about two-thirds the globally derived value. There are three possible explanations: (i) we are witnessing the Local Supercluster at a fortuitous moment in the collapse process, (ii) there is sufficient matter in the disk to constrain the clouds, or (iii) rms random motions are less than 100 km s^{-1} normal to the plane.

Consider the implications of each of these possibilities. In possibility (i), the "fortuitous moment" that is entertained is the epoch of maximum collapse in a dissipationless gravitational clustering scenario. The probability of observing this epoch depends on the velocities that are expected for galaxies as they collapse. If collapse began from an entity that was roughly spherical, then model calculations predict that infall velocities will be well in excess of 1000 km s^{-1} for objects on the scale of the supercluster in full compression today. The system would be confined to $\lesssim 1 h^{-1} \text{ Mpc}$ in one dimension for only 15–20% of the age of the universe. The infall velocities are an order of magnitude larger than the line-of-sight rms velocities of nearby galaxies.

However, the original protostructure (whether composed of galaxies or gas) could not have been strictly spherical because it is observed that the supercluster is expanding in two dimensions while it has collapsed in the third. White and Silk (1979) have studied the development of aspherical structures out of initial homogeneous ellipsoidal density perturbations. They concluded that, if $\Omega \sim 0.1$, the initial fluctuation must have been flattened at least 1.8:1 to explain simultaneously a flattening of 5:1 today, a retardation of the expansion of the Galaxy with respect to the Virgo Cluster of 27%, and a purported measurement of the infall velocity onto the supercluster plane of 280 km s^{-1} . The initial structure must have been flattened at least 3:1 to satisfy these conditions if the universe is marginally closed.

The present observations introduce slightly more stringent constraints. The ratio of the long to short axes of the disk component is at least 6:1, and possibly as large as 9:1. It will be argued in § Vb that the line-of-sight random motions of nearby galaxies are less than 100 km s^{-1} , which might imply that motions toward the plane at our distance from Virgo are less than 170 km s^{-1} .

With models similar to those described by White and Silk (1979), Shaya and I have followed the collapse of families of homogeneous oblate spheroids in an attempt to refine the limits on the flattening required of the initial protostructures. It turns out that the constraints imposed by the axial ratio measurements can be met by only modest ($\sim 20\%$) departures from spherical symmetry, and it is the kinematic constraints which are most severe. Our results are in good accord with those of White and Silk. In universes in which the background can be ignored, models with initial axial ratios greater than 1.5:1 satisfy the observed conditions. Models with initial axial ratios significantly greater than 2:1 are bouncing normal to the plane of the supercluster today, while expansion is only mildly retarded in the plane.

The second suggestion is that galaxies are in rough dynamical equilibrium normal to the plane of the supercluster. By analogy with the classic problem of the z -distribution of material in our Galaxy (cf. Camm 1950), a relationship can be determined between the density of the matter in the plane, ρ_0 ; the scale height of the mass distribution, z_0 ; and the kinetic energy normal to the plane, $v_z^2/2$. Given $\rho(z) = \rho_0 \text{sech}^2(z/z_0)$, then $z_0 = [v_z^2/2\pi G\rho_0]^{1/2}$. A Gaussian scale height, σ_z , was determined for the disk of the Local Supercluster. To a good approximation, $z_0 \approx 1.3 \sigma_z \approx 1.4 h^{-1} \text{ Mpc}$. So, in the case of hydrostatic equilibrium, the density in the plane of the supercluster would be

$$\rho_0 \approx 1.3 \times 10^{-33} v_z^2 h^2 \text{ g cm}^{-3}. \quad (4)$$

There is some convenience to expressing the required mass density in terms of a mass-to-light ratio, utilizing

the observed luminosity density in galaxies. According to the Schechter (1976) luminosity function, galaxies brighter than $-18 + 5 \log h$ are the source of 65% of blue light (given $M^* = -19.5 + 5 \log h$). The number of luminous galaxies and the Gaussian scale lengths in the two clouds which constitute the plane of the supercluster are recorded in Table 1. With this information, the luminosity density in the plane of the supercluster, l_0 , is derived to be

$$l_0 \approx 6 \times 10^9 h L_\odot \text{ Mpc}^{-3}.$$

If the disk is in hydrostatic equilibrium, the mass-to-light ratio in the plane is

$$M/L \approx 30 \left(\frac{v_z}{100} \right)^2 h M_\odot / L_\odot. \quad (5)$$

For convenience, the dependence of M/L on v_z is illustrated in Figure 20.

The third possibility is that random motions perpendicular to the plane are very low. The limit of 100

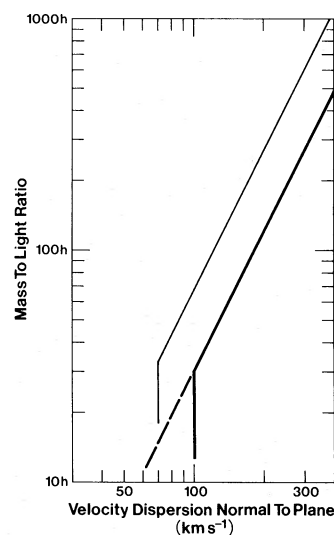


FIG. 20.—The relationship between velocity dispersion normal to the plane and mass density in the plane if the disk is dynamically constrained. The heavy curve illustrates the condition for hydrostatic equilibrium if the scale height is $z_0 \approx 1.4 h^{-1} \text{ Mpc}$. For $v_z \lesssim 100 \text{ km s}^{-1}$ it cannot be argued that the disk is in equilibrium. The light curve is applicable if it is more appropriate to use a local value for the scale height of the plane of $\sim 2/3$ the global value. In that case, either more mass is implied or the constraint on random motions normal to the plane is lowered.

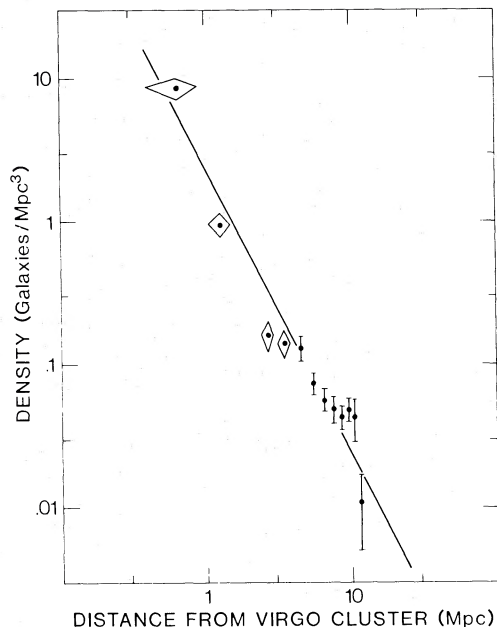


FIG. 21.—The radial distribution of galaxies brighter than $-18 + 5 \log h$ with respect to the Virgo Cluster. Distances have been derived based on the assumption of a uniform expansion. An inverse square dependence of density with distance from Virgo is illustrated.

km s^{-1} to random motions is lower than the collapse or equilibrium motions that would be anticipated through gravitational clustering unless the initial distribution of galaxies was quite flat. If z -motions are so small, the obvious implication is that the disk formed through dissipative processes. In this case, the disk of the Local Supercluster formed before there was significant precipitation into individual galaxies.

V. FURTHER OBSERVATIONAL CONSIDERATIONS

a) The Location of The Virgo Cluster

Given that the Local Supercluster viewed pole-on is so irregular (Fig. 2), one might question whether the Virgo Cluster has a preferred location. In one respect it does in that it is *in the plane* of the Local Supercluster. Moreover, as seen in Figure 21, the number density of luminous galaxies falls off with *distance from the Virgo Cluster squared* (the same dependence was found by Yahil, Sandage, and Tammann 1980, although Jones 1976 concluded the dependence was steeper). It is somewhat surprising that the radial dependence is as well defined as it appears, since, if the equivalents to Figure 21 are drawn for the six separate Virgo-centric quadrants of $2\pi/3$ steradians each, there are order-of-magnitude fluctuations in density with radius. The summation over all angles might have resulted in a radial dependency that is fortuitously smooth, but the conclusion to be

drawn is that the Virgo Cluster is not randomly located within the Local Supercluster.

Nevertheless, the Local Supercluster appears to be asymmetric in that, although the disk scale lengths are $\sim 5 h^{-1}$ Mpc in the directions increasing SGX, decreasing SGX, and decreasing SGY, the scale length is much shorter toward increasing SGY (i.e., beyond the Virgo Cluster in the line of sight). Velocity streaming and sampling effects might be misleading us, but if one uses distances independent of redshifts, the results are qualitatively the same. The drop in density beyond Virgo is faster than expected if the reason is only incompleteness. It is undeniable that there is a large *foreground hole in the plane* of the supercluster. In Figure 9, the only galaxies in the plane with $\text{SGX} < -1 h^{-1}$ Mpc (i.e., foreground of Virgo II) are either in the very nearby Centaurus Group or in the outlying NGC 5643 feature.

b) Independent Evidence for Low Random Motions

While there is a growing conviction that there can be substantial *streaming* motions of entire groups or clouds within the Local Supercluster (e.g., the nearby region is thought to have a non-Hubble motion of several hundred kilometers per second in the general direction of the Virgo Cluster), there is evidence that the *random* motions of individual galaxies that are superposed on large-scale streaming motions are very low. Low random motions in the line of sight would make the proposition of low SGZ-motions more credible.

The histogram of the velocities of nearby galaxies shown in Figure 22 is pertinent evidence. Tammann and Kraan (1978) have argued that the abrupt cutoff at low velocities is a signal that the velocity dispersion with respect to the mean local flow is very low: they claimed that peculiar motions are $25\text{--}50 \text{ km s}^{-1}$! The more complete full-sky sample of NBG merely reinforces these conclusions. There is *no* known galaxy with a blueshift other than among members of the Virgo Cluster and probable members of the Local Group.

It might be proposed that blueshifted galaxies are not observable simply because the Local Group is sufficiently isolated. Essentially all the lowest velocity galaxies are in six nearby groups (Sculptor, IC 342, M81, Centaurus, Canes Venatici I, and M101), so the question is somewhat more complex than would be the case if galaxies were smoothly distributed. There are 88 galaxies in the NBG catalog associated with these six groups.⁵ It is possible to model the expected distribution

⁵Excluding members of the Local Group and the Virgo Cluster, there are only seven galaxies in the NBG catalog with systemic velocities less than 300 km s^{-1} which are *not* in one of these six groups! Four of these are in the south galactic hemisphere, two are in the Leo Minor Cloud, and one is a member of one of the condensed groups of early systems identified in Table 1—the NGC 4274 Group.

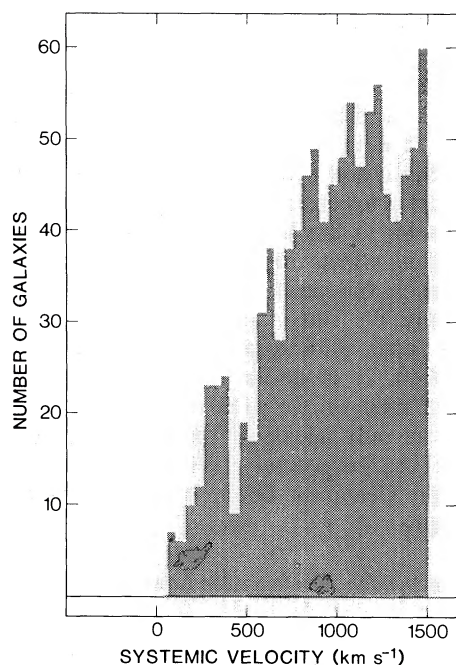


FIG. 22.—The histogram of systemic velocities for all galaxies in the NBG catalog with $V_0 < 1500 \text{ km s}^{-1}$, excluding galaxies associated with the 6° Virgo cluster. The open part of the histogram is contributed by galaxies supposed to be members of the Local Group.

of velocities for these galaxies, assuming any specific value for the dispersion in velocities. Let us suppose that all galaxies identified with a given group are at a common distance. Group distances are taken from non-redshift criteria in an internally consistent system (de Vaucouleurs 1978, 1979). A *local* value of the Hubble constant can be assigned, consistent with the distances assumed ($H_{\text{local}} = 70 \text{ km s}^{-1} \text{ Mpc}^{-1}$). The N_i galaxies associated with the i th group are taken to have a barycentric systemic velocity v_i derived from the assumed distance and H_{local} . It is further assumed that there is a Gaussian distribution in velocities for the galaxies in each group, with the characteristic dispersion to be defined.

The results of models assuming rms velocity dispersions of 50, 100, and 200 km s^{-1} are compared in Figure 23 with the observed velocities for the 88 galaxies in these six groups. Each of the smooth curves derived from the models is normalized such that the integrals under the curves total 88 galaxies. The curve derived from the model with an rms dispersion of 200 km s^{-1} is much too flat compared with the observations, and the curve derived from the 100 km s^{-1} model is unsatisfactory from the same standpoint. The curve consistent with 50 km s^{-1} random motions is qualitatively similar to the observations in terms of amplitudes and the steepness of slopes. Peaks might be displaced in the

models either because of departures from a uniform (local) Hubble flow or through relative distance errors.

As an alternative, it might be conceived that the internal motions within groups can be small but the entire groups have large relative motions. This possibility can be checked by looking at deviations from a *locally* uniform Hubble flow for the six nearest groups, using redshift-independent distances, alternatively, from de Vaucouleurs (1978, 1979: $H_{\text{local}} = 70 \text{ km s}^{-1} \text{ Mpc}^{-1}$) or Sandage and Tammann (1975: $H_{\text{local}} = 55 \text{ km s}^{-1} \text{ Mpc}^{-1}$). I use my own group assignments and redshifts from the NBG, and weight by luminosity to derive group barycentric velocities. Given distances according to de Vaucouleurs, the rms dispersion in the line-of-sight component of group barycentric velocities with respect to a uniform Hubble expansion is only $\pm 15 \text{ km s}^{-1}$. If Sandage and Tammann distances are preferred, then the corresponding dispersion is $\pm 61 \text{ km s}^{-1}$.

The conclusion is drawn that rms random motions within $\sim 4 h^{-1} \text{ Mpc}$ of us are less than 100 km s^{-1} and probably closer to 50 km s^{-1} . All six of the nearest groups are within the Canes Venatici Cloud, so the claim would be that the nearby part of this cloud is streaming as a unit with small internal motions.

Similar conditions are suggested for the other clouds that have been identified. Distances have been derived independent of redshifts to several galaxies in each cloud using the H I profile method (Tully and Fisher 1977). Repeatedly there is evidence that the clouds as a whole are streaming but that the internal random motions are very low. This phenomenon will be explored in a later paper.

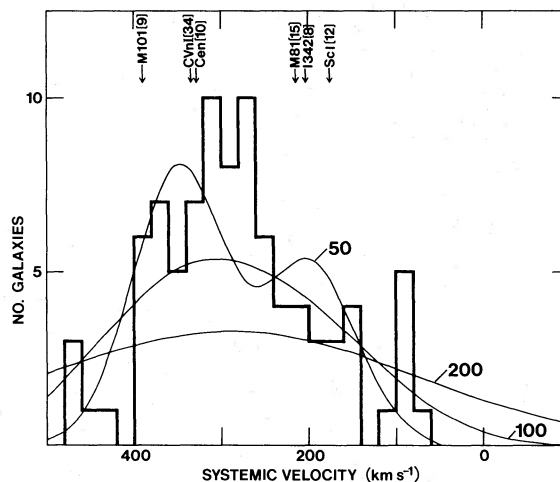


FIG. 23.—A comparison of the distribution of systemic velocities for galaxies in the six nearest groups with models which assume rms random motions of 50, 100, and 200 km s^{-1} . The mean velocities that were assigned to each group and the number of galaxies associated with each group are indicated at the top of the figure.

There is further evidence that small random motions are the rule in the small velocity dispersions associated with loose groups. The well-defined NGC 1023 Group (Tully 1980) provides an example of how remarkably low velocity dispersions can be. In this group, the line-of-sight rms dispersion is only 30 km s^{-1} . In fact, within the redshift of the Virgo Cluster there appear to be only two modest clusters with velocity dispersions exceeding 100 km s^{-1} (Coma I, including the NGC 4274 condensation, and Ursa Major), while there are some two dozen groups with velocity dispersions less than 100 km s^{-1} .

It must be acknowledged that most estimates of peculiar motions have been higher. For example, analyses involving the cosmic virial theorem (Davis, Geller, and Huchra 1978) find one-dimensional velocity dispersions of $\sim 200 \text{ km s}^{-1}$ characteristic of spatially correlated galaxies. A similar value for random motions was found by de Vaucouleurs *et al.* (1981) from velocity residuals using non-redshift distance estimates. The cosmic virial theorem method is vulnerable to departures from spherical symmetry in the distribution of galaxies, and it is evident that such departures are the norm. In any case, earlier estimates have failed to distinguish between streaming and local random motions.

The question of the amplitude of random motions is clearly very important. For the moment, I am content if I have planted a seed of doubt concerning the common occurrence outside rich clusters of local random motions in excess of 100 km s^{-1} .

c) *The Implications if Most of Space Is Empty*

This final point concerns the observed property that the vast majority of galaxies are associated with clouds which occupy only a small fraction of space. Another manifestation of the same property is the observation (Tully and Fisher 1978) that of 412 galaxies with $V_0 < 1100 \text{ km s}^{-1}$, $|b| > 30^\circ$, $\delta \gtrsim -25^\circ$, only *one* system is *further* from its nearest neighbor than the *mean* nearest neighbor separation would be if galaxies were distributed in a cubic lattice.

Of course, it is well established by the covariance studies (Groth and Peebles 1977) that galaxies prefer the company of other galaxies. There has been some success in anticipating the covariance results in terms of gravitational clustering theory (Peebles 1979). It is further claimed that it is not difficult to generate large holes devoid of galaxies in N -body simulations involving only gravitational interactions (Aarseth, Gott, and Turner 1979). However, a universe with large holes is one thing, and a universe which is mostly empty (of luminous matter) is quite another (Einasto, J eveer, and Saar 1980). Admittedly, if closed models of the universe are followed long enough, the contrast between high and low density regions becomes very extreme, and even with open models it is possible by judicious choice of

the initial conditions to freeze structure with qualitative similarities to the filamentary structure found in the Local Supercluster. The challenge to dissipationless clustering theories is the following. *Is it plausible that 98% of the galaxies reside in a small number of clouds* (here, 80% of the galaxies in a volume of $6000 h^{-3} \text{ Mpc}^3$ are in only five clouds) *with 1σ volumes comprising a 5% filling factor?* In particular, can the distribution of galaxies be this clumped and *velocity dispersions still be very low* (Davis *et al.* 1982)?

VI. SUMMARY AND CONCLUSIONS

Attention is drawn to the following characteristics of the nearby overdensity of galaxies referred to as the Local Supercluster:

- i) The vast majority of luminous galaxies reside in a small number of clouds (81% in 5 clouds, 98% in 11 clouds).
- ii) Only 20% of the luminous galaxies are in the Virgo Cluster.
- iii) Averaged over all solid angles, the number density of luminous galaxies falls off as R_v^{-2} , where R_v is the distance from the Virgo Cluster.
- iv) The distribution of galaxies can be described as consisting of two components, one associated with the flattened disk of the Local Supercluster (containing 60% of the luminous galaxies) and the other associated with a roughly spherical "halo" (containing 40% of the luminous galaxies).
- v) The galaxies associated specifically with the halo component are located in a small number of clouds (56% in two clouds, 86% in five clouds, 94% in seven clouds).
- vi) The clouds in the halo are all separated from the supercluster plane by distinct density minima. There are no clouds which intersect the plane of the Local Supercluster.
- vii) The 1σ volume of these clouds occupies only 4% of the total volume off the plane with $|\text{SGZ}| < 10 h^{-1} \text{ Mpc}$ (galactic obscuration has been taken into account in deriving this estimate).
- viii) Almost all the halo clouds can be described as prolate. It appears that the largest three clouds and the CVn Spur are oriented such that their long axes are directed toward the Virgo Cluster. The two most prominent clouds are elongated 2:1.
- ix) On the supposition that this alignment is the consequence of tidal forces that were pronounced when the clouds were forming, an upper limit for the date of this epoch is $z \sim 8$.
- x) The majority of luminous galaxies in the Local Supercluster (60%) are found in the component narrowly confined to a plane. A third of these galaxies are in the Virgo Cluster, and the remainder are assigned to two clouds which can be described as oblate structures in a common plane.

xi) The ratio of the long to short axis for the coplanar component is 6 to 1. These axes are seen largely in projection on the sky, so velocity effects are not significant. This ratio is conservative since the long axis could be underestimated because of galactic obscuration or distance-related incompleteness effects and the short axis could be overestimated through the use of the global value for the disk thickness rather than a mean local value.

xii) Although the intermediate axis is predominantly in the line of sight and velocity effects can be important, there is tentative evidence for a global axial asymmetry in the distribution of galaxies in the Local Supercluster. The falloff in the density of galaxies is seen to be much more rapid on the far side of the Virgo Cluster, and there is a large hole in one quadrant on the foreground side.

xiii) The absolute (global) value of the short axis dimension is $\pm 1.1 h^{-1}$ Mpc (rms dispersion). The plane is actually corrugated, and the local thickness is characteristically about two-thirds the global value.

xiv) For the disk to be this thin, either the Local Supercluster is just now near full collapse, or the disk is constrained by substantial amounts of dark material, or random motions normal to the disk are less than 100 km s^{-1} .

xv) There is independent evidence that local random motions are low in the small dispersion in velocities about a uniform Hubble expansion found among the nearest galaxies and in the low random motions seen in most low-density groups. Line-of-sight random motions are probably less than 100 km s^{-1} and may be much less. This claim is not incompatible with the possibility that major components of the supercluster might participate in streaming motions of several hundred kilometers per second.

These properties of the Local Supercluster can be compared with what is known of somewhat more distant structures. There has been a consistent picture emerging from the studies of the major superclusters at redshifts in the range $3000\text{--}10,000 \text{ km s}^{-1}$: Coma/Abell 1367 (Gregory and Thompson 1978), Perseus (Jöeveer, Einasto, and Tago 1978; Gregory, Thompson, and Tifft 1981), and Hercules (Tarenghi *et al.* 1979). The picture is one of regions rich in galaxies located in sharp contrast with their surrounding volumes, tens of megaparsecs on a side, which are devoid of galaxies. Notably in Perseus, there are elongated structures consisting of chains of clusters, and there is evidence that these large-scale features can be highly flattened. The well-known rich clusters are irregularly embedded in these large-scale entities. This clumpiness in the distribution of galaxies, with superclusters, vast empty regions, and evidence for modest velocity dispersions, has been indicated by other large scale surveys (Kirshner, Oemler, and Schechter 1979; Ford *et al.* 1981; Davis *et al.* 1982).

Similar conclusions are drawn in this study of the Local Supercluster, except that scale lengths are down by an order of magnitude. The three-dimensional distribution is more straightforward to analyze for the nearby structure because the large body of accurate velocities now available allows us to sort out projection effects. Also, with our provident location in the plane of the Local Supercluster, we can make an unambiguous measurement of the thickness of the disk.

The observations must provide support to theories of galaxy and cluster formation that envision large-scale structure to predate structure on the scale of galaxies. The evidence is: the six-to-one flattening of the disk component of the Local Supercluster, the intrinsic thinness of the plane ($\pm 1.1 h^{-1}$ Mpc rms) which may be most plausibly explained in terms of very low random motions normal to the disk ($< 100 \text{ km s}^{-1}$), the extreme segregation of galaxies into clouds which occupy a small fraction of space, and the apparent low local random velocities. This evidence would suggest a scenario of collisions between gas clouds of cluster dimensions or the collapse of gas clouds of such dimensions, followed by radiative dissipation of energy, and fragmentation into galaxies.

Current models invoking asymmetric gravitational collapse of structure on the scale of clusters (Zel'dovich 1970; Sunyaev and Zel'dovich 1972; Icke 1973; Doroshkevich *et al.* 1980*b*) seem qualitatively consistent with the observations. Recent variations of these pancake theories in which neutrinos with finite mass play a dominant role might be favored (Bond, Efstathiou, and Silk 1980; Doroshkevich *et al.* 1980*a*). By contrast if galaxies formed before clusters, as anticipated by the gravitational clustering models which assume the existence of isothermal density fluctuations prior to recombination (Peebles 1974; Aarseth, Gott, and Turner 1979), then it is difficult to understand the efficiency of clustering, the thinness of the disk of the Local Supercluster, and, at the same time, the apparent low random motions. Cosmic turbulence theory as it is presently formulated (Ozernoy 1978) postulates the formation of galaxies before clusters and must face the same criticism.

TABLE 3
LUMINOUS GALAXIES UNASSOCIATED
WITH PRINCIPAL CLOUDS

U3587	
N2549	near Leo Mi
N2775	
N3621	near Antlia
N5301	in CVn Spur
U9242	near CVn Spur
N5984	near Virgo III
N6395	in small cloud centered at $SGX > 10 h^{-1}$ Mpc

TABLE 4
CLOUD ASSIGNMENTS

<i>Canes Venatici</i> : 336 galaxies, 99 luminous galaxies					
0232+59	N 3353	N 3900 L	1204+40	1223+48	N 4861
0238+59	N 3359 L	N 3898 L	N 4121	U 7534	U 8146
U 2847 L	U 5918	N 3913	N 4125 L	N 4414 L	N 4945 L
0355+66	U 5953	U 6816	U 7125	U 7559	U 8188
U 2953 L	U 5979	N 3917 L	N 4136	U 7577	U 8201
N 1569	U 5998	U 6817	N 4138	N 4448	U 8215
N 1560	N 3403 L	U 6818	N 4142	N 4449	U 8246
0427+63	N 3448 L	N 3930	N 4143	U 7599	N 5005 L
U 3203	U 6029	N 3928	N 4145 L	U 7605	U 8261
0509+62	N 3458 L	U 6840	N 4144	N 4455	N 5014
U 3371	U 6161	N 3924	N 4150	U 7608	U 8280
N 2146 L	N 3556 L	N 3938 L	N 4151 L	N 4460	1309+26
0635+75	U 6251	N 3941 L	N 4156	U 7639	N 5023
N 2366	N 3600	N 3945 L	U 7175	N 4485	U 8303
N 2403 L	N 3610 L	N 3949 L	N 4157 L	N 4490 L	N 5033 L
U 4173	N 3619 L	N 3953 L	N 4163	N 4494 L	U 8308
U 4305	N 3631 L	U 6900	U 7207	U 7673	U 8313
0818+71	N 36 L	N 3972 L	N 4173 L	U 7690	U 8320
U 4459	U 6399	U 6912	U 7218	U 7698	U 8323
N 2654 L	N 3657 L	U 6917	N 4183 L	U 7699	U 8331
N 2726 L	N 3675 L	N 3982 L	N 4190	N 4525	U 8333
N 2715 L	U 6446	N 3985	U 7257	U 7719	N 5055 L
N 2742 L	U 6447	U 6923	N 4203 L	N 4534	N 5102
N 2768 L	U 6448	U 6930	N 4204	N 4562	N 5107
U 4841	U 6456	N 3992 L	U 7267	N 4559 L	N 5112 L
N 2787	N 3683 L	N 3990	U 7271	N 4561 L	N 5128 L
U 5139	N 3718 L	N 3998 L	N 4214	N 4565 L	1324-41
N 2950 L	U 6531	U 6955	N 4217 L	U 7774	N 5204
N 2976	U 6534 L	U 6956	N 4218	1236+33	N 5194 L
0946+55	1130+55	N 4010 L	N 4220	N 4605	N 5195 L
N 3027 L	N 3726 L	N 4013 L	U 7300	N 4618	U 8508
N 3031	U 6541	U 6962	N 4236	N 4625	N 5229
N 3034 L	N 3729 L	N 4020	N 4242	U 7866	N 5238
U 5364	N 3733 L	U 6973	U 7321	N 4631 L	U 8578
U 5373	N 3738	1156+46	N 4244	N 4635	N 5236 L
N 3073	N 3755 L	U 6983	N 4245	N 4656 L	N 5253
N 3079 L	N 3756 L	N 4026 L	N 4248	1242+28	U 8651
N 3077	N 3769 L	U 7007	N 4251 L	U 7916	N 5264
N 3109	1135+48	N 4036 L	N 4258 L	N 4670	U 8683
U 5423	N 3782	U 7009	N 4274 L	1243+71	1346-35
U 5455	U 6616	N 4041 L	N 4278	1244+48	U 8760
U 5459 L	U 6628	U 7020	N 4283	1244+26	U 8833
U 5460	1138+35	N 4051 L	N 4288	U 7949	U 8837
1008-04	N 3804	N 4061	N 4293 L	U 7950	N 5408
N 3206 L	N 3813 L	N 4062	U 7408	N 4687	N 5457 L
U 5612	U 6667	N 4068	N 4308	N 4707	N 5474
1023+56	U 6670	N 4065	N 4310	N 4725 L	N 5477
U 5666	U 6682	N 4064 L	N 4314 L	N 4736 L	U 9128
N 3264	U 6706	U 7056	N 4346	N 4747	N 5585
U 5720	U 6713	N 4085	N 4359 L	U 8011	U 9240
N 3252	N 3850	N 4088 L	1222+67	U 8024	U 9405
U 5740	N 3870	U 7089	N 4369 L	U 8036	N 5832
N 3310 L	N 3877 L	N 4096 L	U 7490	N 4800	U 9749
1039+48	1143+35	N 4100 L	N 4389	1253+34	U10822
U 5846	N 3893 L	N 4102	N 4393	N 4826 L	N 6503
U 5848	U 6782	N 4111 L	N 4395	U 8091	N 6946 L

TABLE 4—Continued

<i>Virgo III:</i> 62 galaxies (3 3σ rejections), 41 luminous galaxies					
U 8575	U 9057	U 9249	N 5691 L	U 9500	N 5838 L
U 8614	N 5496 L	U 9275	N 5692 L	N 5750 L	N 5845 L
N 5248	N 5506	N 5638 L	1436-08	1446-09	N 5846 L
N 5300	N 5507 R	U 9310	U 9432	1450-03	N 5854 L
N 5334	U 9169	N 5645 L	N 5701 L	N 5774 L	N 5861 L
N 5348	N 5566 L	N 5669 L	N 5705	N 5775 L	N 5864 L
N 5360	N 5574 L	N 5668 L	N 5713 L	N 5792 L	N 5885 L
N 5363	N 5576 L	U 9380	U 9483 L	N 5806 L	N 5921 L
N 5364	N 5577 L	U 9385	N 5740 L	N 5812 L	N 5964 L
U 8995	N 5584 L	N 5690	N 5746 L	N 5813 L	N 5984 LR
				N 5831 L	U10014 R
<i>Crater:</i> 45 galaxies (3 3σ rejections), 26 luminous galaxies					
N 3585 L	1139-06	1146-28	N 3956	N 4024 L	N 4050 L
N 3637 L	N 3818	N 3904 L	N 3955	N 4027 L	1202-27
N 3672 L	1142-09	N 3923 L	N 3957 L	N 4033 L	1203-27 L
N 3673 L	N 3885 L	N 3936 L	N 3962 L	U 6998 R	N 4094 L
N 3717 L	N 3887 L	1150-03	1152-16	1158-24	1203-22
N 3732	N 3892 L	1150-28	U 6903 R	N 4038 L	N 4105 L
1138-09	U 6780 L	N 3952 L	N 3981 L	N 4039	1210-20
			1155-22	N 4045 LR	N 4462 L
<i>Leo I:</i> 30 galaxies, 15 luminous galaxies					
N 3351 L	N 3384 L	N 3455	N 3507 L	N 3623 L	N 3773
N 3365	N 3412	U 6035	N 3521 L	N 3627 L	N 3810 L
N 3368 L	N 3423 L	N 3489	N 3593	N 3628 L	U 6655
N 3377	N 3447	N 3495 L	N 3605	N 3666 L	U 6670
N 3379 L	U 6007	U 6112	N 3607 L	N 3705 L	N 4037
<i>Leo Minor:</i> 49 galaxies, 11 luminous galaxies					
U 3273	U 4148	U 4514	N 2841 L	N 3115 L	N 3319
U 3475	N 2500	N 2683 L	N 2903 L	N 3184 L	U 5829
N 2337	N 2537	N 2681 L	0930+55	N 3198 L	N 3344 L
U 3817	U 4278	N 2685 L	U 5151	N 3239	U 5889
U 3860	N 2541	U 4704	U 5272	N 3274	N 3432 L
U 3966	N 2552	U 4787	0948+08	U 5740	N 3486 L
U 3974	U 4426	0907-22	U 5340	N 3299	N 3510
U 4115	U 4499	N 2784	N 3104	U 5764	1102+29
					U 6161
<i>Draco:</i> 20 galaxies, 6 luminous galaxies					
U 9211	N 5879 L	U 9893	N 6015 L	N 6239	
N 5608	U 9769	N 5963	U10310	N 6255	
1437+37	U 9776	1535+55	N 6140 L	U10608	
N 5866 L	N 5907 L	U10031	N 6207 L	U10806	
<i>Antlia:</i> 22 galaxies (1 3σ rejection), 6 luminous galaxies					
0834-26	N 2835 L	0931-32	N 2997 L	N 3137	1038-23
0907-33	0919-22	0941-31	N 3056	N 3175 L	N 3511 L
0911-19	0925-31	0942-31	1001-26	1033-24	N 3513 L
		0943-30	N 3113	1033-36	N 3621 LR

TABLE 4—Continued

<i>C Vn Spur</i> : 19 galaxies, 4 luminous galaxies					
N 4861	U 8280	N 5107	U 8489		
U 8246	U 8303	N 5112 L	U 8588		
N 5005 L	N 5033 L	N 5145	N 5273		
U 8261	U 8323	1324+38	N 5301 L		
N 5014	U 8365	U 8449			
<i>Virgo II</i> (southern extension): 122 galaxies, 55 luminous galaxies					
U 6877	N 4420 L	N 4630	N 4713	U 8074	1309-11
N 4030 L	N 4423	N 4632 L	N 4731 L	1255-09	1309-06
U 7053	N 4457	N 4636 L	N 4742 L	N 4845 L	U 8285
N 4116 L	U 7612	N 4643 L	N 4753 L	1256-11	1312-22
N 4123 L	N 4487 L	1241-05	1250-06	N 4856 L	N 5037 L
N 4129	N 4496 L	U 7911	N 4765	1257-12	N 5042
U 7178	1229+04	1242-08	1250-04	N 4880 L	N 5054 L
N 4179 L	N 4504 L	N 4665	N 4772	1258-15	1316-08
1213-11	U 7685 L	N 4666 L	N 4775 L	N 4900	N 5084 L
1214-11	N 4517 L	1243-05	1251-11	N 4941	N 5085 L
U 7332	1230-04	U 7943	N 4781 L	N 4942	N 5087 L
U 7354	N 4527 L	N 4684 L	N 4790 L	1301-03	N 5088 L
N 4260 L	N 4536 L	N 4688	N 4810	1302-075	U 8385
N 4303 L	N 4546 L	N 4691 L	N 4809	1302-073	N 5101 L
N 4324 L	1233-07	N 4697 L	U 8041 L	N 4951 L	1322-19
1220-13	N 4580	1246-04	1252-10	N 4958 L	N 5134 L
N 4339 L	N 4586	N 4699 L	U 8053	1303-17	N 5147
U 7477	N 4592 L	N 4700 L	N 4808	N 4981 L	1323-21
1221+04	N 4594 L	N 4701	N 4818 L	N 4984 L	N 5170 L
U 7512	N 4597	1246-09 L	1254-03	N 4995 L	N 5247 L
				1307-10	1335-09
<i>Leo II</i> : 102 galaxies (5 3σ rejections), 46 luminous galaxies					
0825+52 R	N 2968 L	U 5391	N 3226 L	N 3389 L	U 6258
U 4543	N 2970	U 5393	N 3227 L	N 3395 L	N 3596 L
N 2712 L	0944+39	N 3098	U 5633	N 3396 L	N 3608 L
N 2770 L	U 5245 R	1003+29	U 5662	U 5947	N 3611 L
U 4837	0945+33	U 5478	N 3245 L	N 3414 L	U 6320
N 2778 L	N 3003 L	N 3162 L	U 5675	N 3430 L	N 3626 L
N 2793	N 3011	N 3166 L	N 3254 L	N 3437 L	U 6345
N 2798 L	N 3020 L	U 5522	U 5706	N 3443	N 3630
N 2799	N 3026 L	N 3169 L	U 5708	N 3442	N 3629 L
U 4922 LR	N 3021 L	U 5539	N 3277 L	N 3454	N 3640 L
N 2844	N 3032 L	N 3177	N 3287	1053+06	N 3655 L
N 2852	N 3041 L	1014-03 R	N 3294 L	N 3501	N 3659
N 2853	N 3044 L	N 3185	N 3301 L	N 3504 L	N 3664
N 2859 L	0952+08	N 3187	N 3338 L	N 3512	N 3681
N 2893	0954+33	N 3190 L	U 5833	U 6151	N 3684
N 2955 L	U 5349	N 3193 L	N 3346	U 6171	N 3686 L
N 2964 L	N 3067 L	U 5588	N 3370 L	N 3547	U 6633 R

The program of 21 cm observations that provided much of the data for this study was undertaken jointly with Rick Fisher. The ideas that have been expressed here have been percolating for a sufficiently long while that the list of individuals who should be thanked has become very long. I will only identify Laird Thompson

and Ed Shaya at my own institution as two people who have been especially helpful. It was Herb Rood who provided the inspiration for the cloud numbering scheme in Table 1 through his insistence that the identification of our own cloud, Canes Venatici, is well known. This research was sponsored by NSF grant AST 79-26040.

APPENDIX

In Table 1 of the main text, it was noted that eight luminous galaxies could not be associated with any cloud. These eight galaxies are identified in Table 3.

The cloud assignments given to galaxies in the NBG sample in the vicinity of the Local Supercluster are indicated in Table 4. Systems more luminous than $-18+5 \log h$ are noted by an L. Systems which are in the vicinity of clouds, but which are removed by greater than 3 standard deviations, are noted by an R (these galaxies were *rejected* in the calculation of the cloud dimensions).

In the complete sample volume, $|SGX| < 10 h^{-1}$ Mpc, $0 < SGY < 15 h^{-1}$ Mpc, and $|SGZ| < 10 h^{-1}$ Mpc, among 332 galaxies more luminous than $-18+5 \log h$ there are 88 ellipticals and lenticulars (27%). It is recognized that the rate of occurrence of early morphological types is much higher in more crowded environments. Among 62 luminous galaxies in the 6° Virgo Cluster, there are 34 E and S0 (55%). Among 19 luminous galaxies associated with the three tight condensations identified in Table 1 (the M96, NGC 4274, and NGC 5846 groups), there are 12 E and S0 (63%). Elsewhere in the region of the complete sample, among 251 luminous galaxies there are only 42 E and S0 (17%).

REFERENCES

- Aaronson, M., Huchra, J., Mould, J., Schechter, P. L., and Tully, R. B. 1982, *Ap. J.*, **258**, in press.
- Aaronson, M., Mould, J., Huchra, J., Sullivan, W. T., Schommer, R. A., and Bothun, G. D. 1980, *Ap. J.*, **239**, 12.
- Aarseth, S. J., Gott, J. R., and Turner, E. L. 1979, *Ap. J.*, **228**, 664.
- Bahcall, J. N., and Joss, P. C. 1976, *Ap. J.*, **203**, 23.
- Binney, J., and Silk, J. 1979, *M.N.R.A.S.*, **188**, 273.
- Bond, J. R., Efstathiou, G., and Silk, J. 1980, *Phys. Rev. Letters*, **45**, 1980.
- Camm, G. L. 1950, *M.N.R.A.S.*, **110**, 305.
- Davis, M., Geller, M. J., and Huchra, J. 1978, *Ap. J.*, **221**, 1.
- Davis, M., and Huchra, J. 1982, *Ap. J.*, **254**, 437.
- Davis, M., Huchra, J., Latham, D. W., and Tonry, J. 1982, *Ap. J.*, **253**, 423.
- de Vaucouleurs, G. 1953, *A.J.*, **58**, 30.
- . 1956, *Vistas Astr.*, **2**, 1584.
- . 1975a, in *Stars and Stellar Systems*, Vol. 9, ed. A. and M. Sandage and J. Kristian (Chicago: University of Chicago Press), p. 557.
- . 1975b, *Ap. J.*, **202**, 319.
- . 1975c, *Ap. J.*, **202**, 610.
- . 1975d, *Ap. J.*, **202**, 616.
- . 1976a, *Ap. J.*, **203**, 33.
- . 1976b, *Ap. J.*, **205**, 13.
- . 1978, *Ap. J.*, **224**, 710.
- . 1979, *Ap. J.*, **227**, 729.
- de Vaucouleurs, G., and de Vaucouleurs, A. 1964, *Reference Catalogue of Bright Galaxies* (Austin: University of Texas Press).
- . 1973, *Astr. Ap.*, **28**, 109.
- de Vaucouleurs, G., de Vaucouleurs, A., and Corwin, H. G., Jr. 1976, *Second Reference Catalogue of Bright Galaxies* (Austin: University of Texas Press).
- de Vaucouleurs, G., Peters, W. L., Bottinelli, L., Gouguenheim, L., and Paturel, G. 1981, *Ap. J.*, **248**, 408.
- Doroshkevich, A. G., Khltopov, M. Y., Sunyaev, R. A., Szalay, A. S., and Zel'dovich, Ya. B. 1980a, *Tenth Texas Symposium on Relativistic Astrophysics*.
- Doroshkevich, A. G., Kotok, E. V., Novikov, I. D., Polyndov, A. N., Shandarin, S. F., and Sigov, Yu. S. 1980b, *M.N.R.A.S.*, **192**, 321.
- Einasto, J., Jõeveer, M., and Saar, E. 1980, *Nature*, **283**, 47.
- Fisher, J. R., and Tully, R. B. 1981, *Ap. J. Suppl.*, **47**, 139.
- Ford, H. C., Harms, R. J., Ciardullo, R., and Bartko, F. 1981, *Ap. J. (Letters)*, **245**, L53.
- Gregory, S. A., and Thompson, L. A. 1978, *Ap. J.*, **222**, 784.
- Gregory, S. A., Thompson, L. A., and Tifft, W. G. 1981, *Ap. J.*, **243**, 411.
- Groth, E. J., and Peebles, P. J. E. 1977, *Ap. J.*, **217**, 385.
- Hartwick, F. D. A. 1976, *Ap. J. (Letters)*, **208**, L13.
- Icke, V. 1973, *Astr. Ap.*, **27**, 1.
- Jackson, J. C. 1975, *M.N.R.A.S.*, **173**, 41P.
- Jõeveer, M., Einasto, J., and Tago, E. 1978, *M.N.R.A.S.*, **185**, 357.
- Jones, B. J. T. 1976, *M.N.R.A.S.*, **174**, 429.
- Kirshner, R. P., Oemler, A., and Schechter, P. L. 1979, *A.J.*, **84**, 951.
- Ozernoy, L. M. 1978, in *IAU Symposium 79, The Large Scale Structure of the Universe*, ed. M. S. Longair and J. Einasto (Dordrecht: Reidel), p. 427.
- Peebles, P. J. E. 1974, *Ap. J. (Letters)*, **189**, L51.
- . 1979, *M.N.R.A.S.*, **189**, 89.
- Sandage, A. 1978, *A.J.*, **83**, 904.
- Sandage, A., and Tammann, G. A. 1975, *Ap. J.*, **196**, 313.
- . 1981, *A Revised Shapley-Ames Catalog of Bright Galaxies* (Washington: Carnegie Institution).
- Schechter, P. L. 1976, *Ap. J.*, **203**, 297.
- . 1980, *A.J.*, **85**, 801.
- Shapley, H., and Ames, A. 1932, *Harvard Ann.*, Vol. **88**, No. 2.
- Sunyaev, R. A., and Zel'dovich, Ya. B. 1972, *Astr. Ap.*, **20**, 189.
- Tammann, G. A., and Kraan, R. 1978, in *IAU Symposium 79, The Large Scale Structure of the Universe* (Dordrecht: Reidel), p. 71.
- Tarengi, M., Tifft, W. G., Chincarini, G., Rood, H. J., and Thompson, L. A. 1979, *Ap. J.*, **234**, 793.
- Tonry, J. 1980, Ph.D. thesis, Harvard University.
- Tully, R. B. 1980, *Ap. J.*, **237**, 390.
- Tully, R. B., and Fisher, J. R. 1977, *Astr. Ap.*, **54**, 661.
- . 1978, in *IAU Symposium 79, The Large Scale Structure of the Universe* (Dordrecht: Reidel), p. 31.
- . 1982, *Atlas and Catalog of Nearby Galaxies*, in preparation (NBG).
- White, S. D. M., and Silk, J. 1979, *Ap. J.*, **231**, 1.
- Yahil, A., Sandage, A., and Tammann, G. A. 1980, *Ap. J.*, **242**, 448.
- Zel'dovich, Ya. B. 1970, *Astr. Ap.*, **5**, 84.

R. BRENT TULLY: Institute for Astronomy, University of Hawaii, 2680 Woodlawn Drive, Honolulu, HI 96822